AD-A044 562 DAVID W TAYLOR NAVAL SHIP RESEARCH AND DEVELOPMENT CE--ETC F/G 13/10
COMPONENTS OF FORCE GENERATED BY HARMONIC OSCILLATIONS OF SMALL--ETC(U)
JAN 77 J H PATTISON

UNCLASSIFIED SPD-589-01 NL

| OF |
AD
A044562

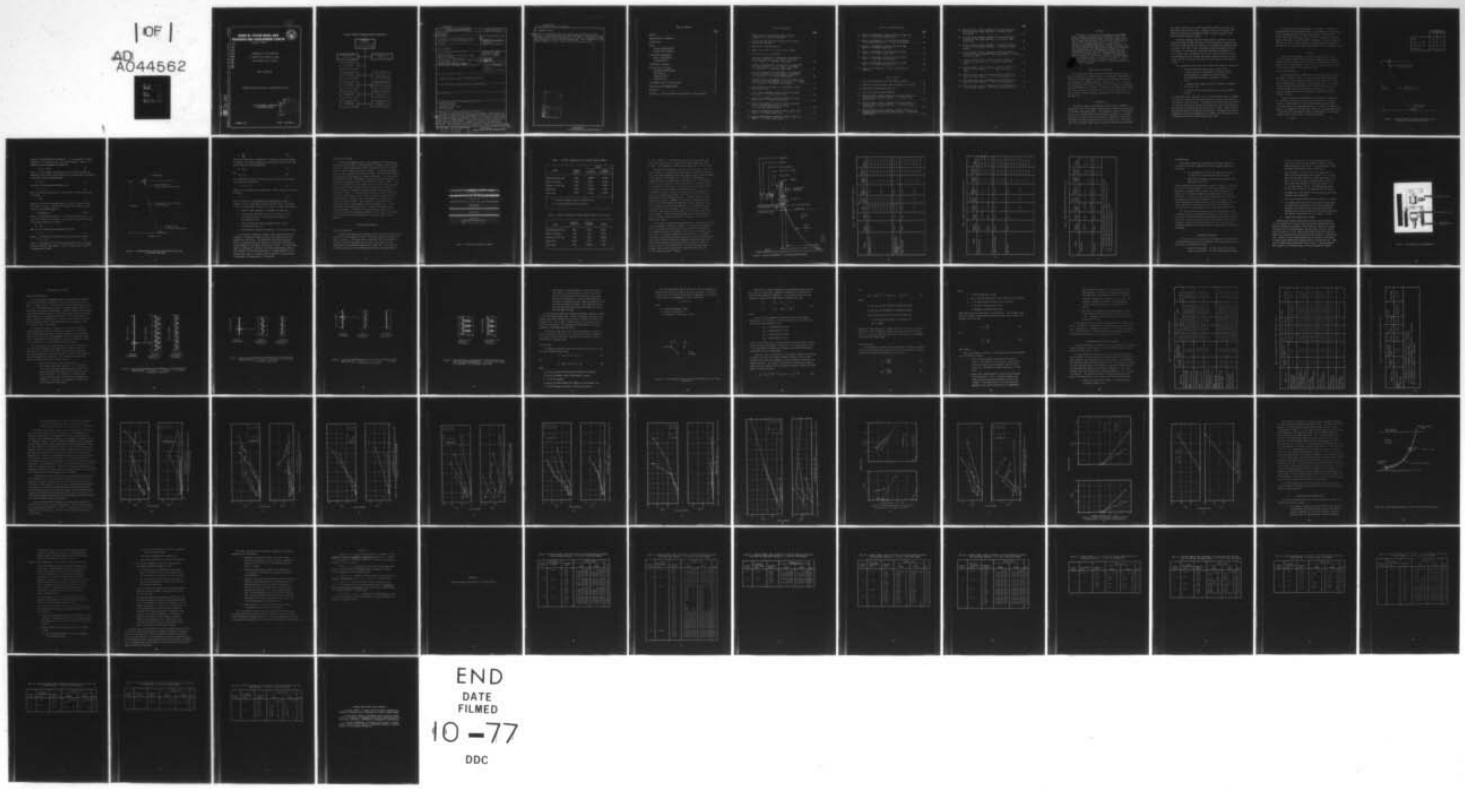

END
DATE
FILMED
10-77
DDC

(12)

DAVID W. TAYLOR NAVAL SHIP RESEARCH AND DEVELOPMENT CENTER

Bethesda, Md. 20084

COMPONENTS OF FORCE GENERATED BY HARMONIC OSCILLATIONS OF SMALL-SCALE MOORING LINES IN WATER

John H. Pattison

SHIP PERFORMANCE DEPARTMENT
DEPARTMENTAL REPORT

JANUARY 1977

REPORT SPD 589-01

MAJOR DTNSRDC ORGANIZATIONAL COMPONENTS

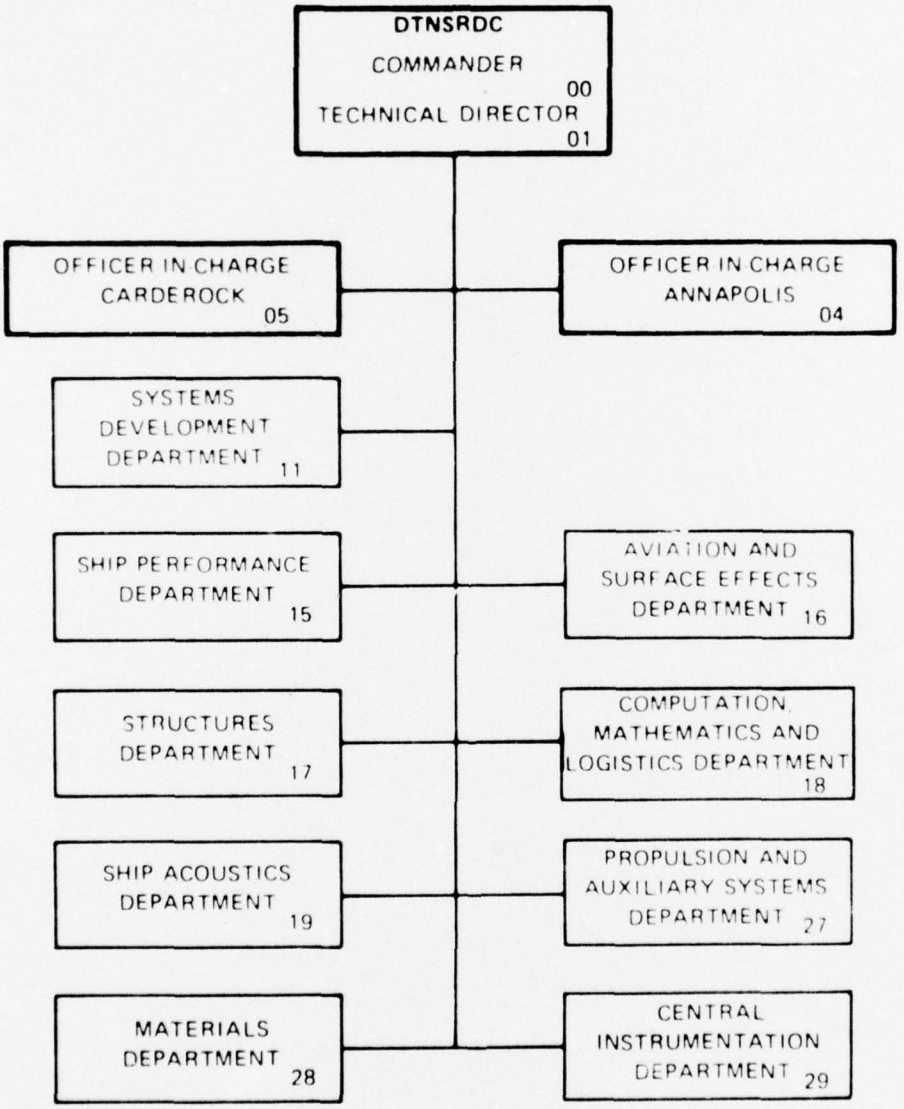

UNCLASSIFIED

SECURITY CLASSIFICATION OF THIS PAGE (When Data Entered)

REPORT DOCUMENTATION PAGE		READ INSTRUCTIONS BEFORE COMPLETING FORM
1. REPORT NUMBER SPD-589-01	2. GOVT ACCESSION NO.	3. RECIPIENT'S CATALOG NUMBER
4. TITLE (and Subtitle) Components of Force Generated by Harmonic Oscillations of Small-Scale Mooring Lines in Water,		5. TYPE OF REPORT & PERIOD COVERED Departmental rept. 6. PERFORMING ORG. REPORT NUMBER SPD 589-01
7. AUTHOR(s) John H. Pattison		8. CONTRACT OR GRANT NUMBER(s)
9. PERFORMING ORGANIZATION NAME AND ADDRESS David W. Taylor Naval Ship Research and Development Center Bethesda, MD 20084		10. PROGRAM ELEMENT, PROJECT, TASK AREA & WORK UNIT NUMBERS NOAA Request H-78003A DTNSRDC W.U. 1548-007
11. CONTROLLING OFFICE NAME AND ADDRESS National Oceanic and Atmospheric Administration NOAA Data Buoy Office National Space Technology Laboratories Bay St. Louis, Mississippi 39520		12. REPORT DATE January 1977 13. NUMBER OF PAGES 63 (270p.)
14. MONITORING AGENCY NAME & ADDRESS(if different from Controlling Office)		15. SECURITY CLASS. (of this report) CLASSIFIED 15a. DECLASSIFICATION/DOWNGRADING SCHEDULE

16. DISTRIBUTION STATEMENT (of this Report)

APPROVED FOR PUBLIC RELEASE: DISTRIBUTION UNLIMITED

17. DISTRIBUTION STATEMENT (of the abstract entered in Block 20, if different from Report)

18. SUPPLEMENTARY NOTES

19. KEY WORDS (Continue on reverse side if necessary and identify by block number)

Moored Buoy Systems
Cable Oscillations
Hydrodynamic Cable Forces
Cable Vibrations

20. ABSTRACT (Continue on reverse side if necessary and identify by block number)

The David W. Taylor Naval Ship Research and Development Center (DTNSRDC) was tasked under the National Oceanic and Atmospheric Administration National Data Buoy Program to conduct an experimental program in the dynamics of mooring lines. Linear scaling of deep-water moorings is impractical and reliance must be made by designers on analytic models. To provide a broad data base applicable to model validation, five small-scale mooring line materials were selected for evaluation. The horizontal and vertical components of dynamic tension generated

next page

DD FORM 1 JAN 73 1473 EDITION OF 1 NOV 65 IS OBSOLETE
S/N 0102-014-6601

UNCLASSIFIED

SECURITY CLASSIFICATION OF THIS PAGE (When Data Entered)

389 694

20. ABSTRACT (cont'd)

by vertical, sinusoidal motion of the upper end of the mooring line were measured. The experiments were made under conditions of current and no current. Data were reduced to force response ratios as a function of frequency of input, and observations of mooring line motions were made. These response ratios were found to depend on preload, current, bending stiffness, and scope.

TABLE OF CONTENTS

LIST OF ILLUSTRATIONS

LIST OF ILLUSTRATIONS (cont.)

LIST OF TABLES

ABSTRACT

The David W. Taylor Naval Ship Research and Development Center (DTNSRDC) was tasked under the National Oceanic and Atmospheric Administration National Data Buoy Program to conduct an experimental program in the dynamics of mooring lines. Linear scaling of deep-water moorings is impractical and reliance must be made by designers on analytic models. To provide a broad data base applicable to model validation, five small-scale mooring line materials were selected for evaluation. The horizontal and vertical components of dynamic tension generated by vertical, sinusoidal motion of the upper end of the mooring line were measured. The experiments were made under conditions of current and no current. Data were reduced to force response ratios as a function of frequency of input, and observations of mooring line motions were made. These response ratios were found to depend on preload, current, bending stiffness, and scope.

ADMINISTRATIVE INFORMATION

This project was established by the National Data Buoy Center, National Ocean Survey, National Oceanic and Atmospheric Administration through the National Aeronautics and Space Administration Defense Purchase Request No. H-78003A, Amendment 2 dated 9 July 1971. The work was accomplished under David W. Taylor Naval Ship Research and Development Center Work Unit 1-1548-007. The draft of this report was prepared prior to the issuance of the directive on the use of metric units. In the interest of time and economy, conversion to the metric units has not been made.

INTRODUCTION

The National Oceanic and Atmospheric Administration (NOAA) is responsible for the development of deep-ocean, moored buoy systems under its National Data Buoy Program. The hydrodynamic aspect of the mooring design is an important part of the moored buoy problem. In a seaway, the mooring is subject to static and dynamic loading from surface and subsurface currents and wave action on the surface buoy. The mooring line and its behavior under current loading and dynamic wave conditions

is a design area which is not well understood although the subject has been under study for many years. Analytic models of the mooring line dynamics problem exist, but data for model validation obtained under controlled conditions are scarce.

In various proposed data buoy system designs, synthetic lines are being considered for deep moorings to reduce the weight for easier handling and to lower mooring line tensions. To minimize the required length of mooring line, short, slack, single-point mooring concepts are being considered. To evaluate and improve the hydrodynamic performance of these systems under development, the David W. Taylor Naval Ship Research and Development Center (DTNSRDC) was tasked by NOAA to conduct an experimental program to provide a data base for use in mooring line dynamics studies.

The experimental program had the following three specific objectives:

1. To provide data on dynamic loads in model mooring lines as functions of frequency to the National Data Buoy Program for validation of analytic methods being developed to predict the dynamics of mooring lines;
2. To determine the ranges over which the dynamic responses are linear; and
3. To observe any non-linear effects, such as out-of-plane motions.

The experiments were conducted in the Circulating Water Channel at DTNSRDC. Five material samples were selected to provide a broad range of mooring line physical characteristics. The experimental mooring lines were varied in scope and subjected to forced vertical harmonic oscillation applied at the upper end to simulate the vertical motion of a buoy. Other variables were current speed and frequency of oscillation. Horizontal and vertical components of tension were measured at the upper end of the mooring line, and observations of the response motions were made.

In this report the scaling problem is discussed. It should be emphasized that the experimental models do not represent a scaled model of any proposed design for the Data Buoy Program. They have been chosen to provide a data base having sufficient variation in key parameters to be useful in analytic model validation. The report contains descriptions of the models, apparatus and procedures and presents the data both in the form of corrected measurements and force response ratios.

MODELS

With existing technology, a deep sea mooring cannot be scaled in the Circulating Water Channel. However, experiments on a variety of mooring line materials can provide data to validate the analytical models over a limited range. Thus, in this section, scaling considerations and descriptions of the models are given.

SCALING CONSIDERATIONS

Three typical mooring concepts for the National Data Buoy System are shown in Figures 1 and 2. In terms of conventional buoy mooring definitions, all three concepts are short, slack mooring lines with various combinations of synthetic line and anchor chain. The scopes of these systems are greater than one so they are slack but only a fraction greater than one, so they are relatively short. Here, scope is defined as the ratio of equilibrium mooring line length to depth of water.

To obtain ideal experimental data for validation of the design, the mooring lines should be scaled for both geometric and elastic similarity, and appropriate scaling laws should be applied to the full-scale current and sea-state conditions. In Breslin's analytical model,[2,3] the equations of motion for transverse and longitudinal waves in a mooring line are properly scaled if Froude number is maintained constant, where Froude number is defined as follows:

$$F = U/(g\ell)^{1/2} \qquad (1)$$

	Configuration	
	A	B
Scope	1.13	1.3
Dacron line (ft)	1,641	1,641
Nylon Line (ft)	11,960	14,109
Chain (ft)	180	180

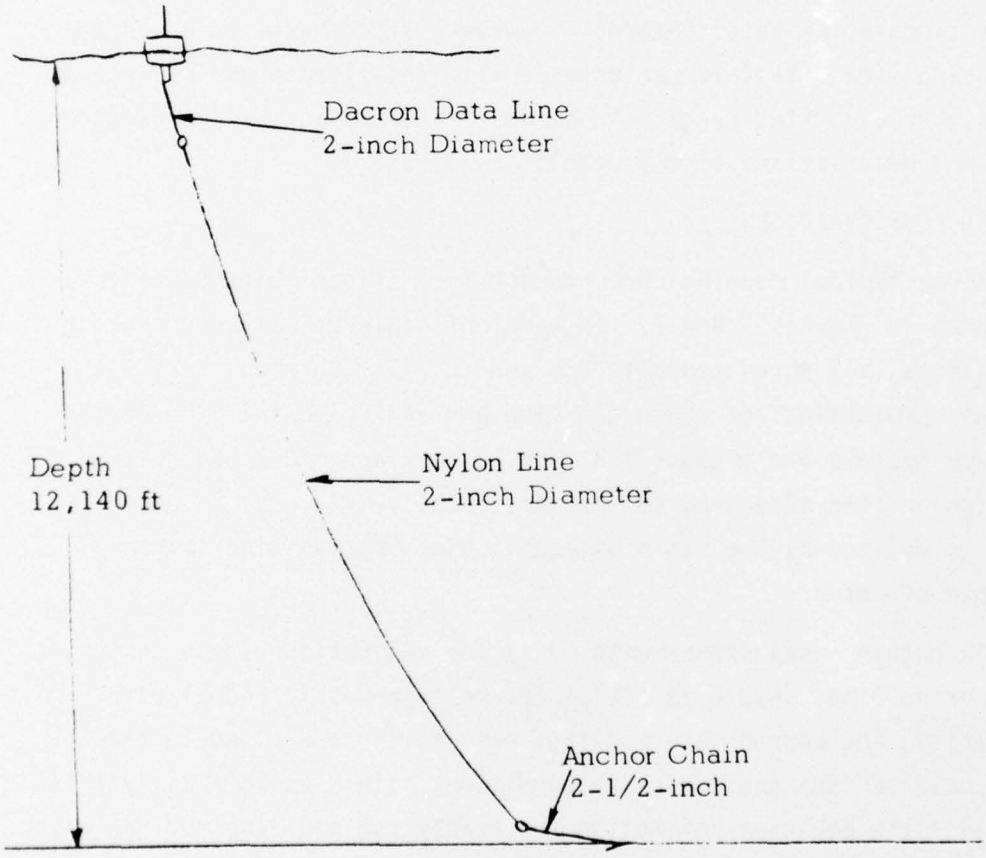

Figure 1 - General Dynamics, Electronics Division Mooring Concepts for the National Data Buoy

where g is acceleration due to gravity, ℓ is a characteristic length (diameter or line length), and U is current velocity. Hence, if a geometric scaling parameter is defined as

$$\lambda = \ell_p/\ell_m = d_p/d_m \tag{2}$$

where d is line diameter and subscripts m and p refer to model and prototype, respectively, then Froude scaling relates model to prototype velocities by the following equation

$$U_m = U_p/\lambda^{1/2} \tag{3}$$

and model to prototype wave frequencies by

$$f_m = \lambda^{1/2} f_p \tag{4}$$

Breslin expresses the celerity (or wave speed) of longitudinal waves as follows[3]

$$K = \left(\frac{AE}{\mu}\right)^{1/2} \tag{5}$$

where A is line cross sectional area, E is Young's modulus of the line material, and μ is mass per unit length of the cable; and the celerity of transverse waves as

$$C = \left\{\frac{T_o}{(1+\varepsilon_o)\mu'}\right\}^{1/2} \tag{6}$$

where T_o is equilibrium tension, ε_o is equilibrium strain, and μ' is the virtual mass per unit length. Now, Froude scaling relates model to prototype area by the following

$$A_m = A_p/\lambda^2 \tag{7}$$

Mass per unit length may be expressed as follows

$$\mu = \rho_c A \tag{8}$$

where ρ_c is the density of the mooring line; and virtual mass as

$$\mu' = (\rho_c + \rho)A \tag{9}$$

where ρ is the density of the fluid and the mooring line is assumed to have a circular cross section. Also, the equilibrium strain may be expressed as follows

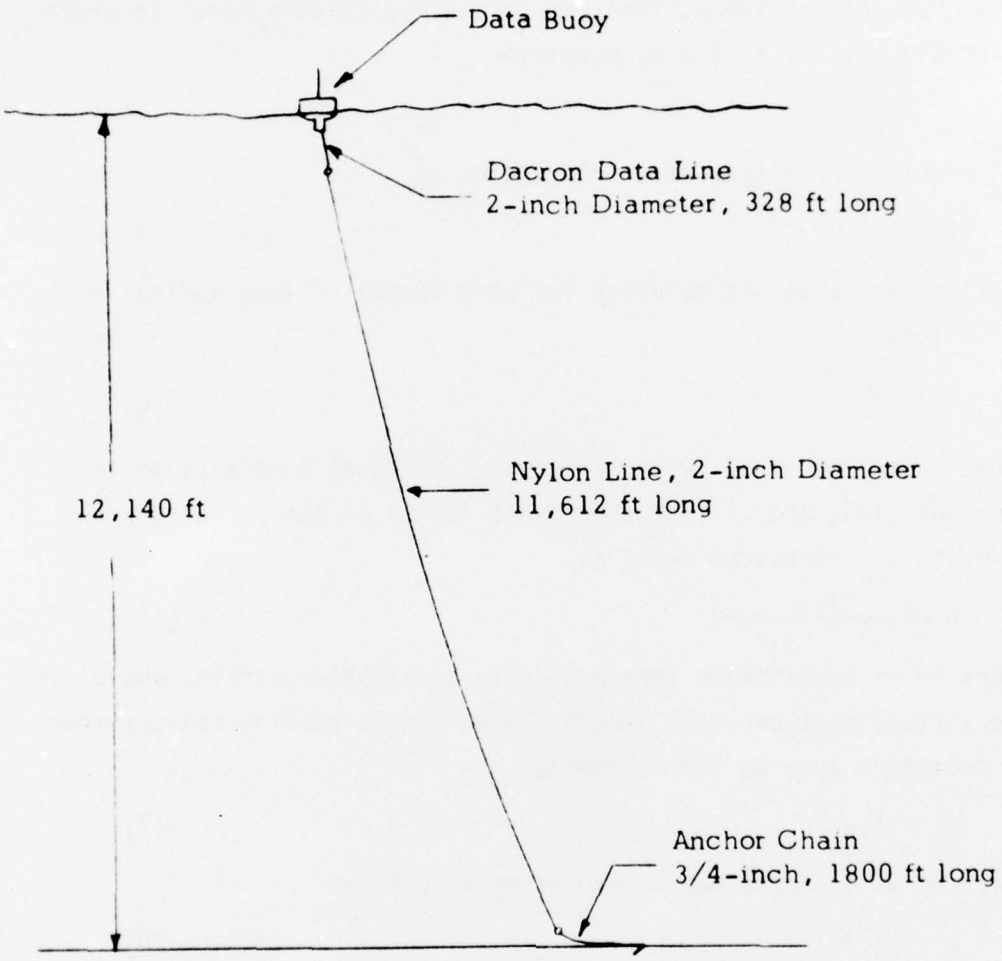

Figure 2 - Lockheed Missiles and Space Company Mooring Concept
For National Data Buoy

$$\epsilon_o = \frac{T_o}{AE} \tag{10}$$

Since, by Froude scaling, equations (5) and (6) will scale according to equation (3), Young's modulus and line material density are found to scale by the following equations

$$E_m = E_p/\lambda \tag{11}$$

and

$$\rho_{cp} = \rho_{cm} \tag{12}$$

Now, hydrodynamic forces on the buoy which transmit into the mooring line take the following form

$$T = \tfrac{1}{2}\, \rho U^2 A \;\; C_T \tag{13}$$

where C_T is a constant, force coefficient. Hence, forces scale by the following

$$T_m = T_p/\lambda^3 \tag{14}$$

Hence, to scale the 12,140-foot mooring depth designs shown in Figures 1 and 2 or even their shallow, 3280-foot depth, counterpart in the Circulating Water Channel with a depth of 9 feet would require:

1. Mooring lines comparable in diameter to a human hair,
2. Input motion amplitudes of a small fraction of an inch at frequencies 20 or so times the wave frequencies encountered at sea,
3. Current speeds less than one-twentieth the currents encountered at sea, and
4. Instrumentation capable of measuring in the milligram range.

For economy and expediency, these scaling requirements were not attempted. Conventional model scaling of real deep-sea moors was judged to be impractical. The experiments herein were designed primarily through selection of materials to provide a data base for the development and validation of analytical models. If an analytical model can reproduce the results of controlled experiments, even on short lengths of line, then confidence in its applicability to full-scale mooring lines is increased, and the problem of linear scaling of deep-moors for design data is circumvented.

DESCRIPTION OF MODELS

To match the assumptions used in the mathematical representations for predicting the dynamic loads and motions in mooring lines, an ideal material for model experiments would be completely flexible in bending and would have a smooth, cylindrical surface.[2] To provide measurable tensions, the line also would have to be heavy. No material was readily available which would meet all of these requirements. As a result, the five sample materials illustrated in Figure 3 were chosen arbitrarily. The physical characteristics of the samples are listed in Table 1. The relative acceptability of the samples in terms of three physical characteristics are listed in Table 2 to permit comparison. The open link chain is flexible in bending and heavy; but does not have a smooth cylindrical surface. The mercury filled tube has a smooth cylindrical surface and medium weight, but is stiff in bending and tends to kink. The bead chain is flexible, but is light weight and does not have a smooth cylindrical surface. The wire rope is nearly smooth and cylindrical, but is light weight, stiff, and tends to kink. On the other hand, the weighted nylon cord is flexible, smooth and cylindrical, and heavy. In addition, the nylon cord has extensibility similar to that of the prototype synthetic mooring lines. The weighted nylon cord is most like the synthetic lines used in the full-scale moorings.

EXPERIMENTAL ARRANGEMENT

MODEL CONFIGURATIONS

The model experiments were conducted in the Circulating Water Channel[4] which has a working depth of 9 feet. The general mooring arrangement is shown in Figure 4. The lower end of the mooring line was secured to a tie-down block on the bottom, with the upper end secured to a two-dimensional force dynamometer mounted on a slider arm. The slider arm is driven vertically in a sinusoidal motion with a fixed amplitude of

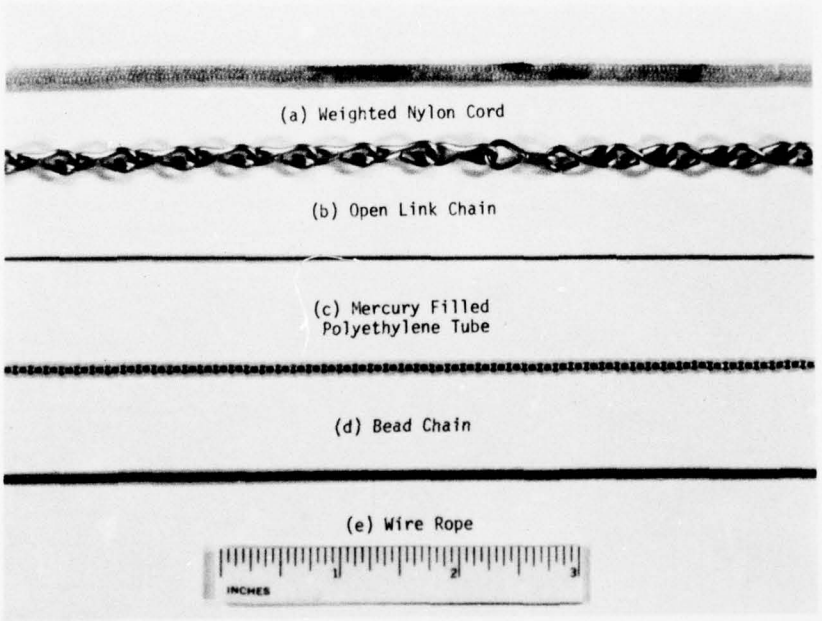

Figure 3 - Model Mooring Material Samples

TABLE 1 - PHYSICAL CHARACTERISTICS OF MODEL MOORING SAMPLES

Sample	Diameter, Inches	Weight	
		Air, Pounds/Foot	Water, Pounds/Foot
Weighted Nylon Cord	0.128	0.0264**	0.0194
Open Link Chain	0.195*	0.0417	0.0362
Mercury Filled Tube	0.067	0.0100	0.0086
Bead Chain	0.056*	0.0068**	0.0051
Wire Rope	0.069	0.0075	0.0064

* *Effective diameter based on projected area.*

** Includes absorbed or entrained water.

TABLE 2 - RELATIVE SIMILARITY OF MODEL MOORING SAMPLES TO FULL-SCALE

Sample	Bending Flexibility	Surface Smoothness	Weight
Weighted Nylon Cord	Good	Good	Heavy
Open Link Chain	Good	Poor	Heavy
Mercury Filled Tube	Poor	Good	Medium
Bead Chain	Good	Poor	Light
Wire Rope	Poor	Average	Light

0.5 inch (0.043 ft). A motor driven pivot arm and cable were used to pull the slider arm up. Negator springs were used to pull the arm down. The frequency of motion was variable from 0.1 to 2.2 hertz.

The experimental conditions for the five model mooring lines are given in Table 3. Listed are the model material, anchoring configuration, water depth spanned, mooring line length, scope, motion amplitude, current speed, and the preset trail (horizontal displacement (x)) between the upper and lower ends of the mooring line. The upper-end termination was mounted on a movable carriage which allowed horizontal displacement to be varied. The mooring line lengths were selected to correspond to the typical full scale scopes of 1.1 and 1.3 illustrated in Figure 1, except for the case of the weighted nylon cord which exceeded these values. The length of the nylon line was computed rather than measured directly. In water, nylon parachute cord normally shrinks. However, in this case, the shrinking nylon tended to neck down between the lead balls used to weight the line, which resulted in their being pushed apart. This extended the line 1.25 percent over its dry length. Also, the nylon cord exhibited an elastic coefficient (spring constant of a unit length under load) of 36.5 pounds. These two factors together with the average dynamic tension value were used to compute the "stretched" length from the measured dry length.

With respect to the anchoring configuration, fixed-pivot or "excess line on-the-bottom" cases are indicated. For "excess on-the-bottom" cases, a reference was established at the specified line length and this reference was set just tangent to the channel floor under steady conditions. The current speeds were 0 and 0.6 knots. The preset horizontal displacement positions were established from previous experiments and from the calculation of conditions where the steady horizontal force-component at the top would be 0.25 and 0.5 times the weight in water of the mooring line. The resulting steady loads, however, deviated from these desired loads and ranged from 0.05 to 0.85 times the weight in water.

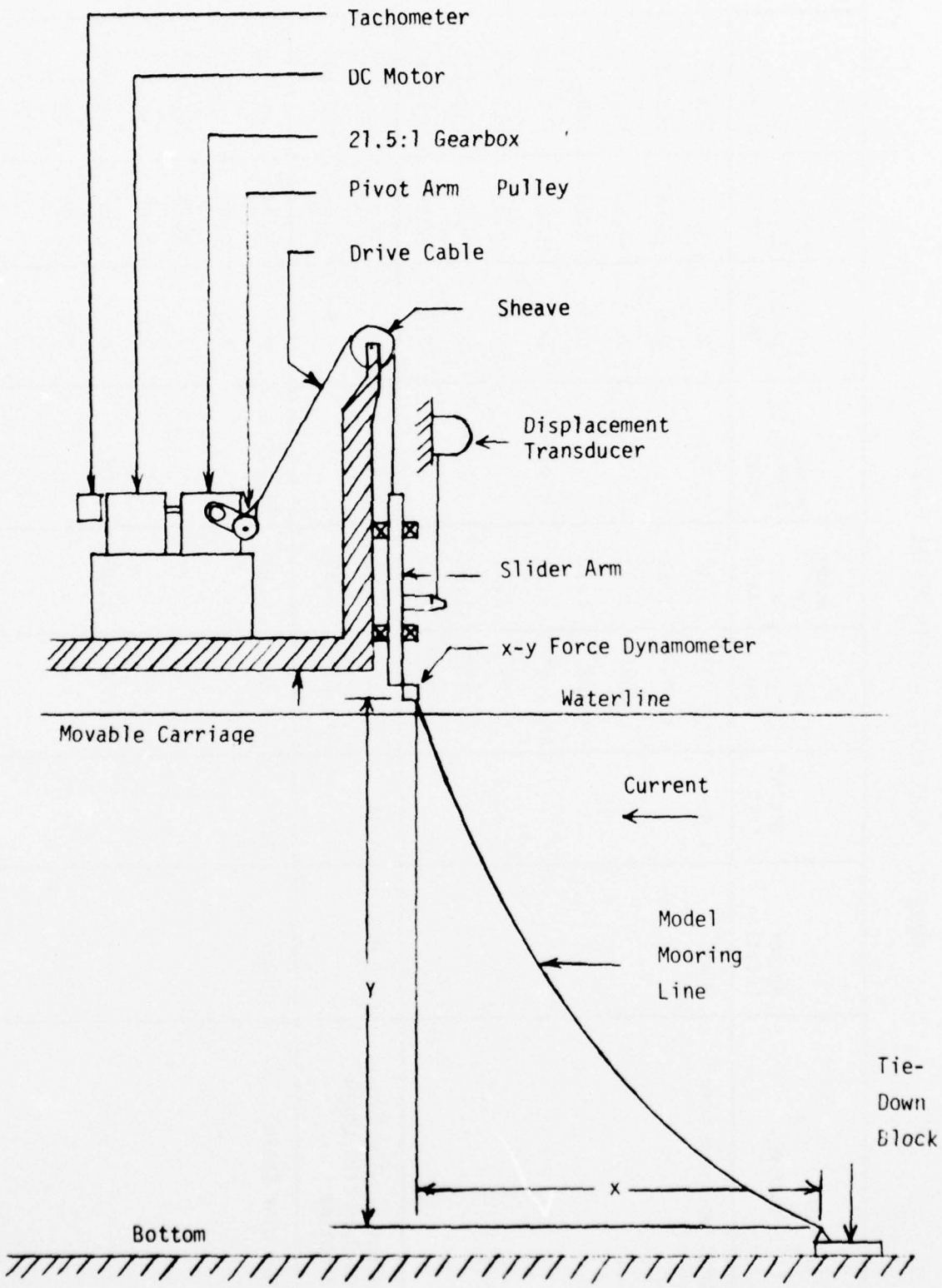

Figure 4 - Mooring Arrangement in Circulating Water Channel

TABLE 3 - MODEL MOORING EXPERIMENTAL CONDITIONS

Sample	Anchor Location	Depth,* Feet	Line Length,* Feet	Scope To Depth Ratio	Motion Amplitude, Feet	Current Speed, Knots	Preset Trail,* Feet	Run Numbers
Weighted Nylon Cord	Pivot	9.00	10.05**	1.12	0.043	0	3.76	148-151
			10.08**	1.12		0.6	3.69	152-155
			10.05**	1.12		0	4.02	156-159
			10.09**	1.12		0.6	3.81	160-163
			11.89**	1.32	0.043	0	6.23	113-116
			11.93**	1.33		0.6	6.61	117-120
			11.89**	1.32		0	7.04	121-143
			11.92**	1.33		0.6	6.88	144-147
Weighted Nylon Cord and Open Link Chain on Bottom	Bottom	9.04	12.20***	1.35	0.043	0	6.78	196-199
			12.23***	1.35		0.6	5.63	200-203
Open Link Chain	Pivot	9.00	9.90	1.10	0.043	0	3.76	43- 49
						0.6	3.69	50- 56
						0	4.02	57- 61
						0.6	3.79	62- 68
			11.70	1.30	0.043	0	6.23	164-167
						0.6	6.61	168-171
						0	7.04	172-175

TABLE 3 - MODEL MOORING EXPERIMENTAL CONDITIONS (cont.)

Sample	Anchor Location	Depth,* Feet	Line Length,* Feet	Scope To Depth Ratio	Motion Amplitude, Feet	Current Speed, Knots	Preset* Trail, Feet	Run Numbers
Open Link Chain	Pivot					0.6	6.88	176-179
		9.05****	12.29	1.36	0.109	0	7.05	120-128****
						0.6	7.05	129-133****
	Bottom	9.04	12.05***	1.33	0.043	0	6.72	29- 35
						0.6	5.73	36- 42
Mercury Filled Tube	Pivot	9.00	10.0	1.11	0.043	0	3.80	97-100
						0.6	3.73	101-104
						0	4.06	105-108
						0.6	3.85	109-112
Bead Chain	Pivot	9.00	9.90	1.10	0.043	0	3.76	81- 84
						0.6	3.69	85- 88
						0	4.02	89- 92
						0.6	3.81	93- 96
			11.70	1.30	0.043	0	6.23	180-183
						0.6	6.61	184-187
						0	7.04	188-191
						0.6	6.88	192-195

TABLE 3 - MODEL MOORING EXPERIMENTAL CONDITIONS (cont.)

Sample	Anchor Location	Depth,* Feet	Line Length,* Feet	Scope To Depth Ratio	Motion Amplitude, Feet	Current Speed, Knots	Preset* Trail, Feet	Run Numbers
Bead Chain								
	Bottom	9.04	12.05***	1.33	0.043	0	6.38	69- 72
						0.6	2.82	73- 76
			14.50***	1.60	0.043	0.6	8.88	77- 80
Wire Rope	Pivot	9.00	9.90	1.10	0.043	0	3.76	15- 21
						0.6	3.69	22- 28

* Cable dimensions include approximately 0.04 foot of cable above water surface.

** Stretched length which includes both wet stretch and extension under load.

*** Line Length does not include line lying on bottom.

**** Conditions from high amplitude experiments.

INSTRUMENTATION

The parameters measured in addition to the characteristics of the mooring line models themselves and their catenary configurations were:

1. The components of force in the upper end of the line in the vertical and horizontal directions, and
2. Amplitude and frequency of the vertical motion at the upper end of the line.

The two component force dynamometer is shown in Figure 5. Each load cell has a 2.2-pound capacity. A special signal control unit energized the force gages and the return signal was displayed on a Sanborn 320 strip chart recorder and a Weston Model 1240 Digital Multimeter. On the strip chart record, resolution to ± 0.05 pound was obtained; on the digital multimeter, to ± 0.01 pound. The force measurements were complicated by interaction between the horizontal and vertical force gages and inertia of the dynamometer. These effects were accounted for by calibration as explained later.

The input motion was measured by a linear displacement transducer whose signal was recorded on a Sanborn 322 strip chart recorder. The vertical force signal was recorded alongside the linear displacement signal to obtain the phase relationship between force and motion. Frequency of motion input was measured to within ± 0.01 hertz by a tachometer attached to the motor shaft and a Weston Model 1240 Digital Multimeter.

EXPERIMENTAL PROCEDURE

The first task in the experimental procedure was to establish the pre-experimental equilibrium configuration of the model mooring line, and it was accomplished as follows:

1. Anchor Configuration - The lower end of the line was secured to the anchor. In cases where the mooring was

to have a fixed pivot, the line was attached to the pivot pin on top of the tie-down block shown in Figure 4. Where some mooring line was to lie on the bottom, it was attached to the bottom of the tie-down block.

2. Anchor Position - For the fixed pivot cases, the tie-down block was positioned on the channel floor in alignment with two cross references. Where some mooring line was to lie on the bottom, a reference mark on the line was aligned with reference lines on the channel floor. In this case several feet of line separated the anchor and the point of mooring line tangency with the bottom.

3. The upper end of the mooring line was attached to the two component load dynamometer.

4. The current flow was established at either 0 or 0.6 knots.

5. The steady-state configuration was established by moving the upper end of the mooring line on the carriage downstream until the desired configuration was obtained. Reference marks on the channel wall were used to determine the mooring line terminal points to within ± 1/8-inch.

6. Steady-state forces were recorded.

After the equilibrium configuration had been set and recorded, vertical harmonic oscillation of the upper end was established at the desired frequencies, and dynamic input motion and loads were recorded. Throughout most of the experiments, the amplitude of vertical motion remained fixed at 0.5 inch. Movies were taken through the surface to observe any out-of-plane motions (normal to the current) in the mooring line. Movies also were taken through the side windows in the channel to observe both standing and traveling waves in the mooring line. Both types of observations yielded qualitative results. These procedures were repeated for different preset locations and material samples.

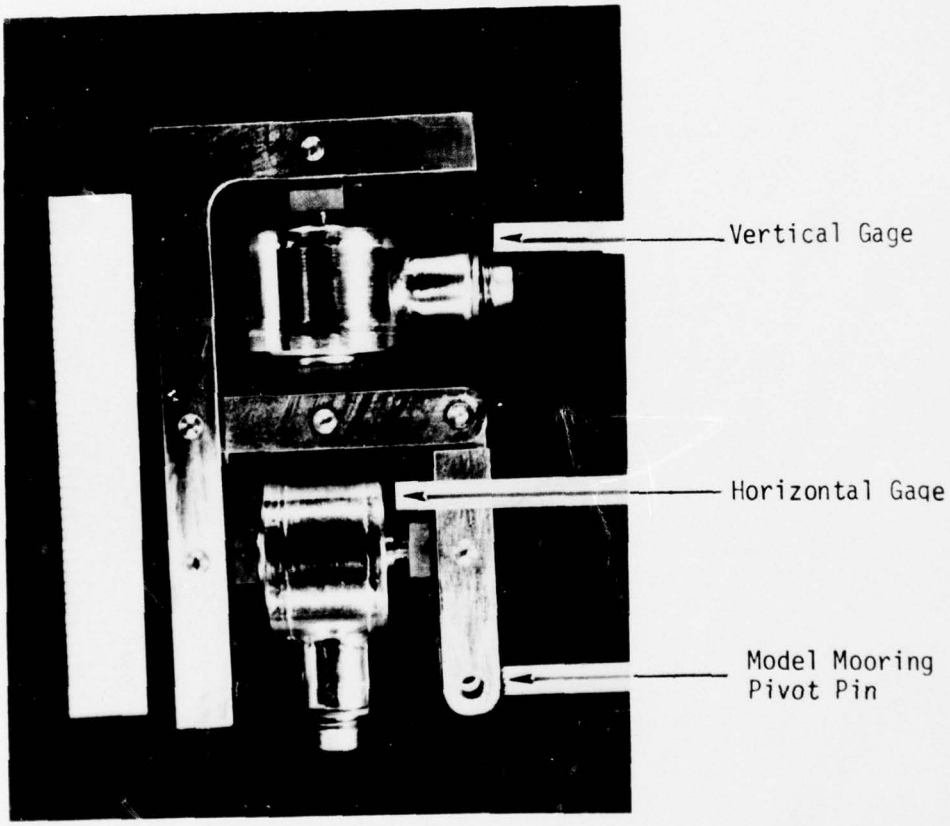

Figure 5 - Two Component Force Dynamometer

DATA REDUCTION TECHNIQUE

WAVEFORM CONSIDERATIONS

Typical load and displacement traces from the Sanborn 320 and 322 strip chart recorders are shown for the case of the open-link chain model in Figures 6 and 7 (fixed pivot anchor with scope-to-depth ratios of 1.1 and 1.3 respectively) and Figure 8 (scope-to-depth ratio of 1.3 and excess chain lying on the bottom). Figure 6 represents the shortest scope condition which results in the highest dynamic loads and the most distorted signals, although this distortion is not strong enough to prevent analysis of these data as if they were pure sinusoidal signals. Small amplitude ripples on the signal may be due to pendulus motion of individual links in the chain.

The load traces shown in Figures 6, 7, and 8 do not represent pure horizontal and vertical forces because there are significant interactions between the gages in the two component force dynamometer. Also, inertia loads from the dynamometer itself are present in these traces. Methods for eliminating these interactions and inertia loads from the data analysis are discussed in the next section.

The load traces for the other models are similar to Figure 6, 7, and 8 but are of generally lower magnitudes. However, under some conditions the load traces are highly distorted in that they show sharp spikes that peak to much higher maximum loads than are observed when the responses are sinusoidal. The following two distinctly different conditions result in distorted loads:

1. Models with smallest scope-to-depth ratios ($\delta = 1.1$) and highest preset trail distances ($x = 3.79$ feet at $U = 0.6$ knot) have the highest tensions of any of the models when the slider which drives the line is at the top of its travel. This results in distorted load traces, especially when the amplitude or frequency is increased. An example is illustrated in Figure 9 for for the open-link chain model.

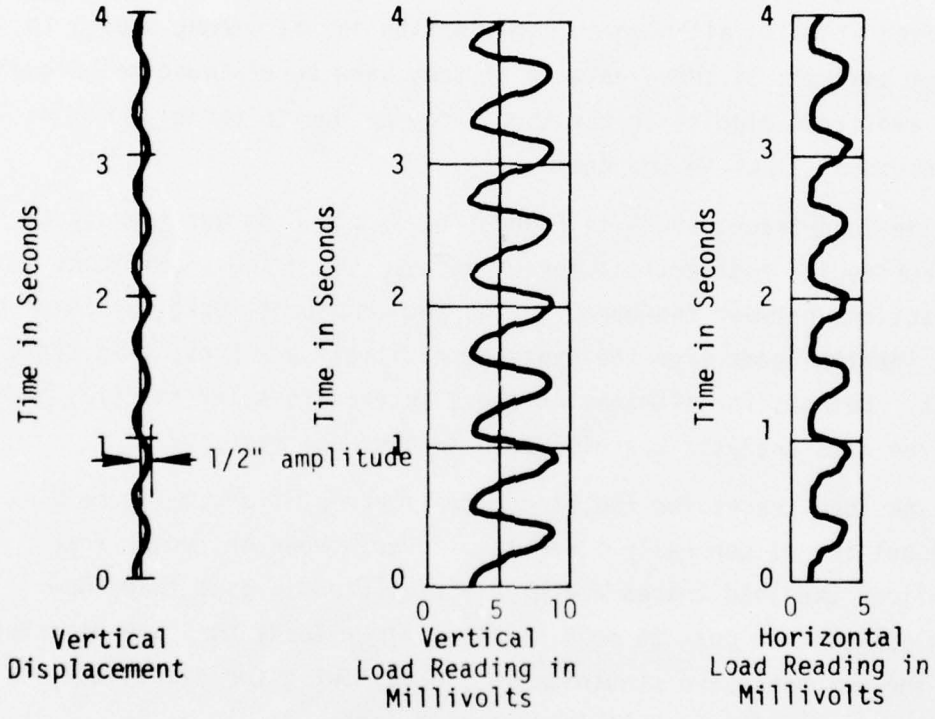

Figure 6 - Vertical Displacement and Load Records on an Open-Link Chain Model Mooring; ℓ = 9.9 Feet, U = 0.6 Knots, x = 3.79 Feet, f = 1.84 Hertz, Fixed Pivot

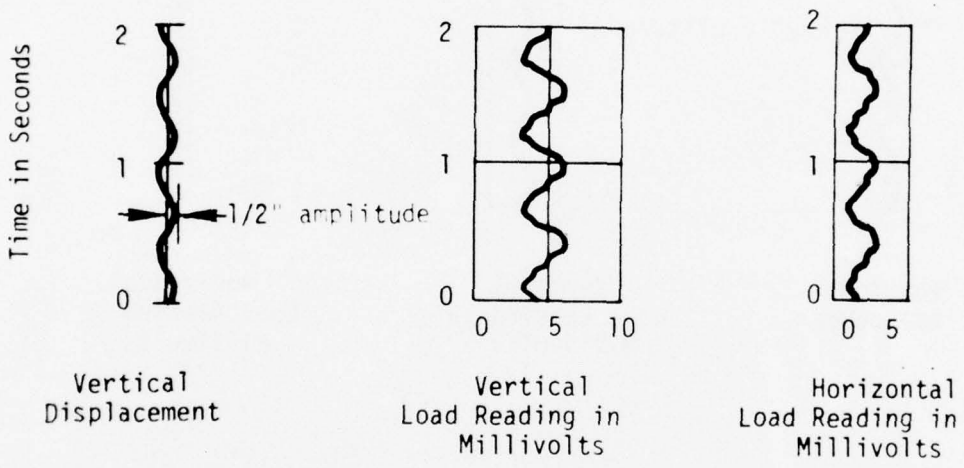

Figure 7 - Vertical Displacement and Load Records on an Open-Link Chain Model Mooring; ℓ = 11.7 Feet, U = 0.6 Knots, x = 6.88 Feet, f = 1.82 Hertz, Fixed Pivot

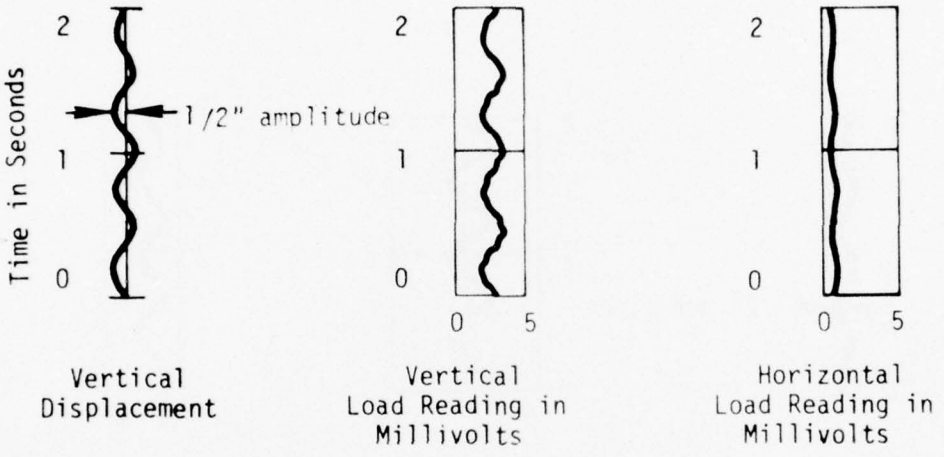

Figure 8 - Vertical Displacement and Load Records on an Open-Link Chain Model Mooring; ℓ = 12.05 Feet, U = 0.6 knots, x = 5.73 Feet f = 1.81 Hertz, Bottom Anchor

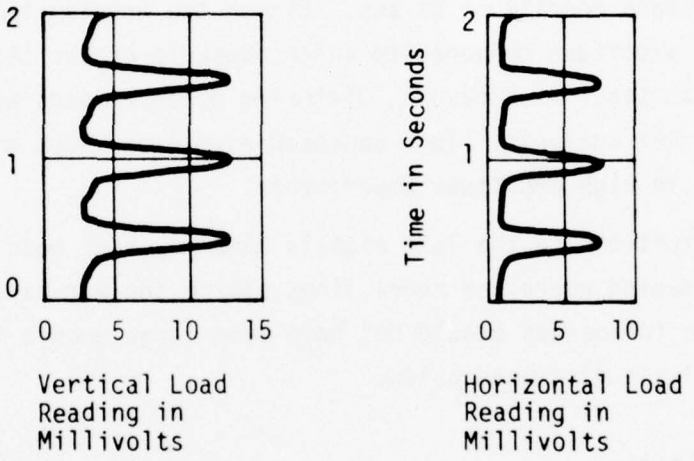

Figure 9 - Distorted Dynamic Load Response to Vertical Motion on an Open-Link Chain Model Mooring; ℓ = 9.9 Feet, U = 0 Knots, x = 4.02 Feet, f = 1.30 Hertz, Fixed Pivot

2. When subject to high amplitude (0.109 foot instead of 0.043 foot) all mooring models go slack at the lower position of the slider and then snap up as the slider moves to its top position. In the high amplitude experiments, the resulting "snap" loads were observed to be sensitive to bending stiffness. The relatively stiff wire rope exhibited more severe snap loads than did the flexible open-link chain.

In any case, the above two conditions represent unrealistic models of full-scale conditions at sea. Either the mooring is tauter or the motional amplitude compared to water depth is higher than those anticipated at sea. As a result, distorted dynamic loads were ruled out from further analysis. This approach eliminated most of the data gathered in high amplitude experiments.

Distortions in the load signals also may have been influenced by uneven loading where the model lines pierce the air-water interface, but these influences should not have been large enough to effect the data analysis discussed below.

DATA ANALYSIS

The tension components contain both equilibrium and dynamic terms and may be expressed as follows:

$$T_x = T_{0x} + F_x \sin(\omega t + \phi_x) \tag{15}$$

and

$$T_y = T_{0y} + F_y \sin(\omega t + \phi_y) \tag{16}$$

where

T_{0x} and T_{0y} are equilibrium tension components in pounds,

F_x and F_y are dynamic tension amplitudes in pounds,

t is time in seconds,

ϕ_x and ϕ_y are phase angles with respect to displacement, and

ω is the frequency of motion in radians per second.

The sign conventions used to define the forces (components of tension) and motion of the top of the cable are shown in Figure 10. T_x and T_y are the horizontal and vertical components of the tension in pounds and y is displacement in feet, of the form

$$y = a \sin \omega t \tag{17}$$

where

a is motion amplitude in feet,

t is time in seconds, and

ω is frequency in radians per second.

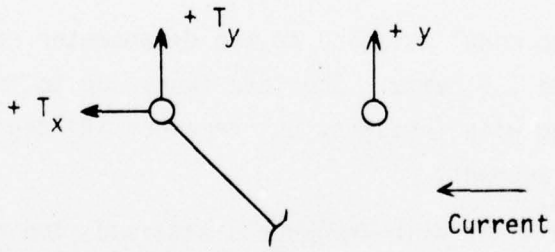

Figure 10 - Sign Conventions for Loads and Displacement of Top of Model Mooring Line

Calibration of the two component load dynamometer revealed strong but linear and predictable interactions between the horizontal and vertical force measuring components. So, to obtain forces from the measured voltages, the following matrix equation was used:

$$\begin{pmatrix} T_x \\ \\ T_y \end{pmatrix} = \begin{pmatrix} a_{xx} & a_{xy} \\ \\ a_{yx} & a_{yy} \end{pmatrix} \begin{pmatrix} V_x \\ \\ V_y \end{pmatrix} \qquad (18)$$

where

V_x and V_y are the measured horizontal and vertical voltages, respectively, in millivolts. From the calibrations, the interaction coefficients were determined to be

$$a_{xx} = 0.1854 \text{ pounds/millivolt}$$

$$a_{xy} = -0.0616 \text{ pounds/millivolt}$$

$$a_{yy} = 0.1876 \text{ pounds/millivolt}$$

$$a_{yx} = -0.0632 \text{ pounds/millivolt}$$

Dynamic calibrations with mo model attached to the dynamometer revealed significant tare loads above 1.5 hertz. The tare loads due to inertia in the dynamometer increased with frequency but remained 180 degrees out-of-phase with the displacement.

Under oscillating conditions with the models attached, the measured horizontal and vertical voltages remained in phase with each other, although their phase relationships to the displacement varied with different conditions. As a result, the following equations were used to remove the tare voltages from the measured voltages to obtain corrected dynamic voltage amplitudes.

$$V_{dx} = \left[V_{xm}^2 \sin^2 \theta + (V_{xm} \cos \theta - V_{xt})^2 \right]^{1/2} \qquad (19)$$

and

$$V_{dy} = \left[V_{ym}^2 \sin^2 \theta + (V_{ym} \cos \theta - V_{yt})^2 \right]^{1/2} \qquad (20)$$

where

V_{dx} and V_{dy} are the corrected voltage amplitudes,

V_{xm} and V_{ym} are the measured voltage amplitudes,

V_{xt} and V_{yt} are the tare voltage amplitudes, and

θ is the phase angle between the measured and tare voltages.

Because of higher resolution, voltages read from the digital voltmeter were used in the data analysis rather than readings from the Sanborn charts. V_{dx} and V_{dy} then were substituted into Equation (18) to obtain the dynamic force amplitudes.

RESPONSE RATIOS

In the mathematical models under development to predict the dynamic load and motion responses of moorings,[2] the dynamic loads may be obtained from non-dimensional coefficients, which follow:

$$C_{fx} = \frac{F_x/T_0}{\omega\, a/U} \qquad (21)$$

$$C_{fy} = \frac{F_y/T_0}{\omega\, a/U} \qquad (22)$$

where

a is motion amplitude in feet,

F_x and F_y are horizontal and vertical dynamic load in pounds,

T_0 is the measured equilibrium tension in pounds,

U is current in feet per second, and

ω is frequency in radians per second.

These coefficients are zero when no current exists. So, to obtain some comparison between current and no-current conditions the following load response ratios are used:

$$R_{fx} = \frac{F_x}{T_0} \tag{23}$$

and

$$R_{fy} = \frac{F_y}{T0} \tag{24}$$

ERROR ANALYSIS

Overall resolution, or accuracy, of the data analysis was dependent upon the following factors:

1. Vertical and horizontal voltages were accurate to within ± 0.05 millivolt. As a result, resolution of equilibrium vertical and horizontal loads is 0.006 pound, and, cumulatively, tension resolution is 0.009 pound.

2. Phase angles between dynamic voltage and displacement were accurate to ± 10 or ± 20 degrees depending on signal amplitude and paper speed on the strip chart recorder. The uncertainties in the load amplitude depended on this angle variance and also depended on

the relative magnitudes of the measured dynamic and tare voltages. As a result, the uncertainty in the load amplitude varied depending on the run condition.

3. Tachometer voltages were measured to ± 0.5 volt. As a result, frequency resolution is 0.004 hertz and circular frequency resolution is 0.024 radian per second.

4. With flow in the channel at 0.6 knot, speed is maintainable and uniform from surface to floor to within ± 10%. However, speed did not enter into the calculations which follow.

In the data analysis, the above resolutions were included as error terms. For example, in Equation (18), the voltage V_x was written as $V_{xm} \pm \delta V$ where V_{xm} is a measured voltage and δV is voltage resolution (δV = 0.05 millivolt). The final results are tabulated in Appendix A in terms of values plus or minus cumulative error limits.

EXPERIMENTAL RESULTS AND DISCUSSION

The calibration matrix of Equation (18) was applied to the measured steady voltages to obtain steady loads on the mooring models. These results are summarized in Table 4.

The tare correction Equations (19) and (20) and the calibration matrix Equation (18) were applied to the measured cynamic voltages to obtain dynamic load amplitudes on the mooring models. For comparison with analytical predictions, Equations (23) and (24) were used to transform the load amplitudes into horizontal and vertical response ratios. The load amplitude results are tabulated in Appendix A. The load response ratios are plotted versus reduced frequency ω a/c in Figures 11 through 22. The results are shown in order of decreasing confidence in the data, which is influenced by the following two factors:

1. Similarity of the sample materials as model moorings as noted in Table 2, and

TABLE 4 - EQUILIBRIUM LOADS ON MODEL MOORINGS

Model Type	Current*, Knots	Horizontal** Displacement, Feet	T_{ox} *** Pounds	T_{oy} *** Pounds	T_o **** Pounds	$T_{ox}/w\ell$	Run Number
Weighted Nylon Cord ℓ = 10.05 to 10.08 Feet Fixed Pivot Anchor	0	3.76	0.050	0.200	0.206	0.26 ± 0.03	148-151
	0.6	3.69	0.019	0.343	0.344	0.10 ± 0.03	152-155
	0	4.02	0.062	0.212	0.221	0.32 ± 0.03	156-159
	0.6	3.81	0.010	0.372	0.372	0.05 ± 0.03	160-163
Weighted Nylon Cord ℓ = 11.89 to 11.93 Feet Fixed pivot anchor	0	6.23	0.062	0.212	0.221	0.27 ± 0.03	113-116
	0.6	6.61	0.059	0.346	0.351	0.26 ± 0.03	117-120
	0	7.04	0.112	0.237	0.262	0.49 ± 0.03	121-143
	0.6	6.88	0.099	0.349	0.363	0.44 ± 0.03	144-147
Weighted Nylon Cord with open-link chain on the bottom ℓ = 12.20 to 12.23 Feet Bottom Anchor	0	6.78	0.093	0.268	0.284	0.34 ± 0.02	196-199
	0.6	5.63	0.012	0.312	0.312	0.04 ± 0.02	200-203
Open-Link Chain ℓ = 9.9 Feet, fixed pivot anchor	0	3.76	0.075	0.449	0.455	0.21 ± 0.04	43- 46
	0.6	3.69	0.072	0.634	0.638	0.20 ± 0.04	50- 53
	0	4.02	0.199	0.699	0.726	0.56 ± 0.04	57- 59
	0.6	3.79	0.112	0.762	0.770	0.31 ± 0.04	62- 65
Open-Link Chain ℓ = 11.7 Feet Fixed pivot anchor	0	6.23	0.081	0.456	0.463	0.19 ± 0.03	164-167
	0.6	6.61	0.124	0.574	0.587	0.29 ± 0.03	168-171
	0	7.04	0.233	0.570	0.616	0.55 ± 0.03	172-175
	0.6	6.88	0.196	0.658	0.687	0.46 ± 0.03	176-179

TABLE 4 - EQUILIBRIUM LOADS ON MODEL MOORINGS (cont.)

Model Type	Current* Knots	Horizontal** Displacement Feet	T_{ox}*** Pounds	T_{oy}*** Pounds	T_{o}**** Pounds	$T_{ox}/w\ell$	Run Number
Open-Link Chain ℓ = 12.05 Feet Bottom Anchor	0 0.6	6.72 5.73	0.087 0.038	0.437 0.487	0.445 0.488	0.20 ± 0.03 0.09 ± 0.03	29- 32 36- 39
Polyethylene Tube filled with Mercury, ℓ = 10.0 Feet Fixed Pivot Anchor	0 0.6 0 0.6	3.80 3.73 4.06 3.85	0.019 0.031 0.043 0.047	0.094 0.106 0.118 0.209	0.095 0.111 0.126 0.214	0.22 ± 0.07 0.07 ± 0.07 0.50 ± 0.07 0.55 ± 0.07	97- 98 101-104 105-106 109-112
Bead Chain ℓ = 9.9 Feet Fixed Pivot Anchor	0 0.6 0 0.6	3.76 3.69 4.02 3.81	0.012 0.015 0.043 0.040	0.062 0.153 0.094 0.178	0.063 0.154 0.103 0.182	0.24 ± 0.26 0.30 ± 0.26 0.85 ± 0.26 0.79 ± 0.26	81- 82 85- 86 89- 90 93- 94
Bead Chain ℓ = 11.7 Feet Fixed Pivot Anchor	0 0.6 0 0.6	6.23 6.61 7.04 6.88	0.034 0.028 0.043 0.047	0.047 0.090 0.069 0.109	0.058 0.095 0.081 0.119	0.57 ± 0.11 0.47 ± 0.11 0.72 ± 0.11 0.79 ± 0.11	180-183 184-187 188-191 192-195
Bead Chain ℓ = 12.05 Feet Bottom Anchor	0 0.6	6.38 2.82	0.031 -0.019	0.056 0.056	0.064 0.059	0.50 ± 0.10 -0.31 ± 0.10	69- 70 73- 74
Bead Chain ℓ = 14.5 Feet Bottom Anchor	0.6	8.88	0.006	0.081	0.081	0.08 ± 0.08	77- 78

TABLE 4 - EQUILIBRIUM LOADS ON MODEL MOORINGS (cont.)

Model Type	Current* Knots	Horizontal** Displacement Feet	T_{ox} *** Pounds	T_{oy} *** Pounds	T_o **** Pounds	$T_{ox}/w\ell$	Run Number
1/16-inch Aircraft Cable ℓ = 9.9 Feet	0	3.76	0.025	0.075	0.079	0.39 $\pm$ 0.10	15- 18
	0.6	3.69	0.031	0.206	0.208	0.49 $\pm$ 0.10	22- 25

* Uncertainty in flow speed at 0.6 knot is ± 0.06 knot.

** Uncertainty in horizontal displacement is ± 0.01 foot.

*** Uncertainty in x and y components of tension is ± 0.006 pound.

**** Uncertainty in tension is ± 0.009 pound.

2. Uncertainties and inaccuracies in the data as discussed in the Error Analysis Section. The resulting uncertainties also are listed in the data tables in Appendix A.

The effects of preload, flow and scope on the dynamic load response ratios also are shown in Figures 11 through 21. The dependence on frequency of the dynamic load response ratios on the weighted nylon cord are little affected by preload, as illustrated in Figures 11 and 12. However, Figures 14 and 15 illustrate increases in this dependence for the response ratios with increasing preload on the open-link chain. A similar effect is illustrated in Figures 18 and 19 for the bead chain. However, Figure 17 illustrates increasing response ratios with no flow and decreasing response ratios with flow on the mercury filled tube. Figures 13, 16, 20, and 21, cases where portions of the line were lying on the bottom, could not be considered to illustrate the effects of preload because in these cases preload could not be varied without changing the scaope. The differences in effects of preload may be due to differences in the bending stiffness. The open-link chain and bead chain are extremely flexible in bending, whereas the weighted cord is slightly stiff and the mercury filled polyethylene tube is stiffest.

To determine the effects of current on the dependence on frequency load response ratios, care must be taken to look only at cases where equilibrium $T_{ox}/w\ell$ is nearly the same for flow and no flow conditions. With this in mind, Figures 12, 14, 18 and 19 illustrate that the effect of current is to increase the load response ratios for the weighted cord, the open-link chain, and the bead chain. Similar preload conditions were not obtained for the mercury-filled tube. As a result, no interactions between the effects of stiffness and the effects of current on the load response ratios were observed.

Increasing scope tends to decrease the load ratios, especially when some of the line is lying on the bottom. This is illustrated for the weighted cord, the open-link chain, and the bead chain in Figures 11 through 16 and 18 through 21. Results for the tube are limited to a single scope.

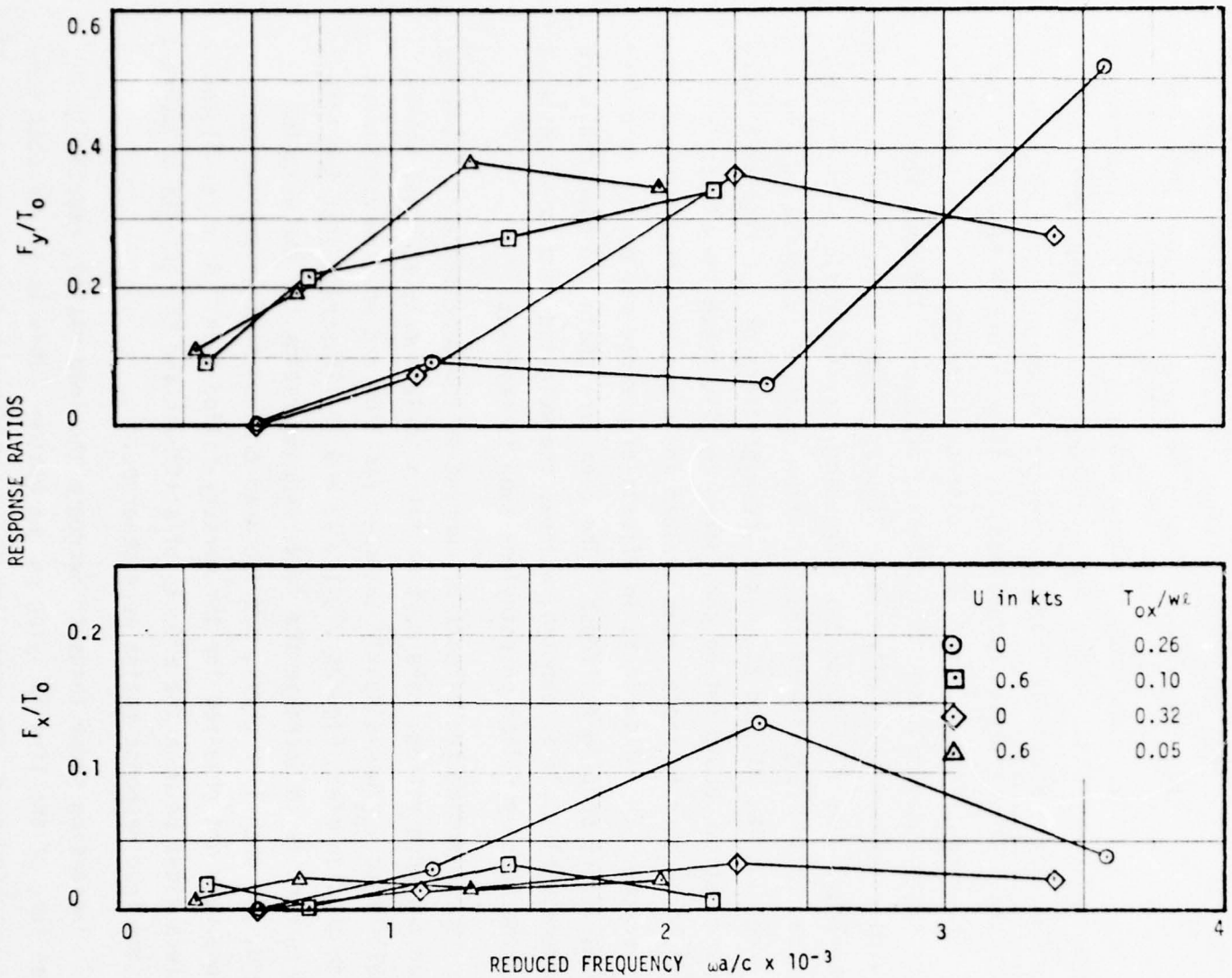

Figure 11 - Dynamic Load Response to Vertical Motion on Weighted Nylon Cord
(ℓ = 9.9 feet, Fixed Pivot)

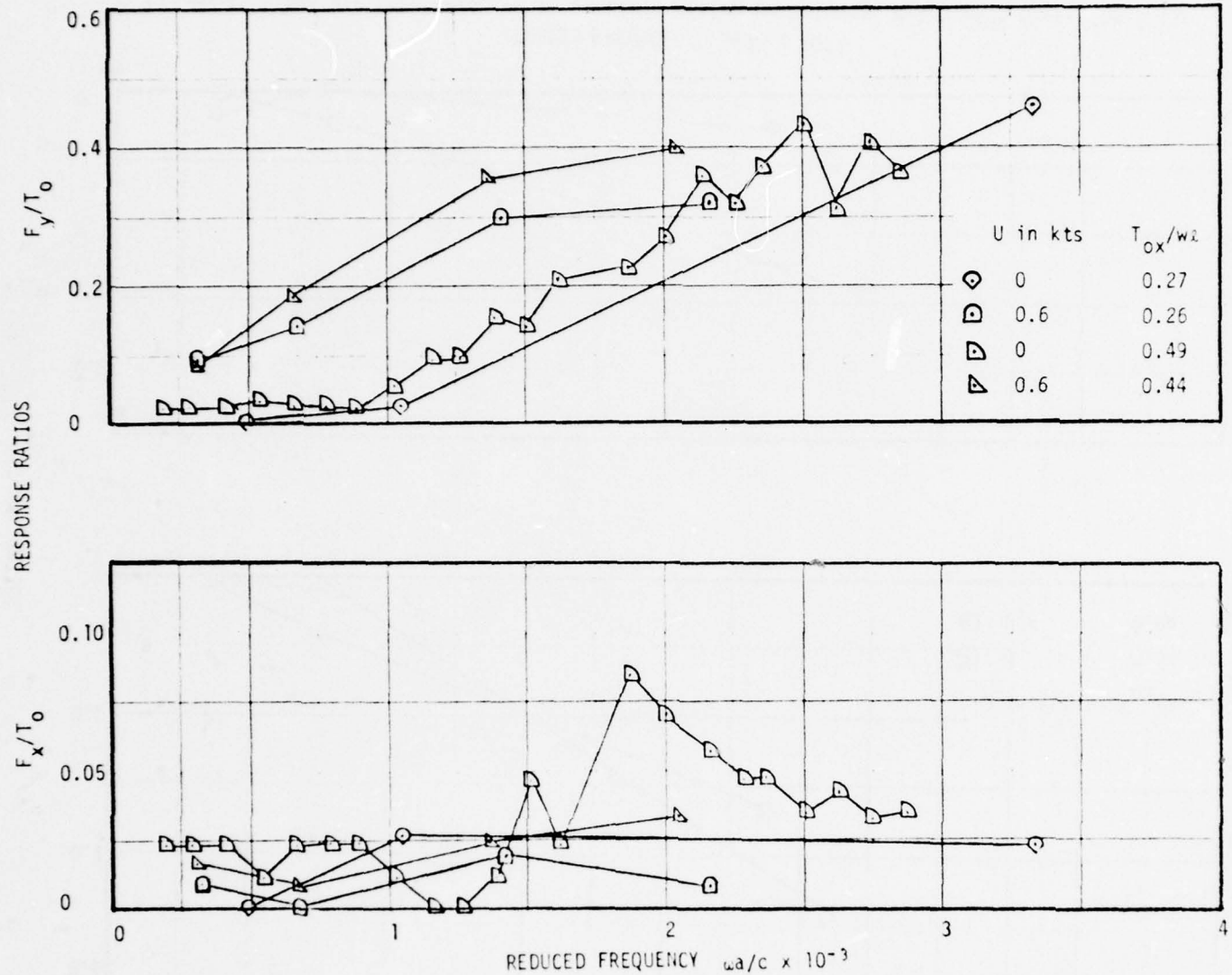

RESPONSE RATIOS

Figure 12 - Dynamic Load Response to Vertical Motion on Weighted Nylon Cord
(ℓ = 11.7 feet, Fixed Pivot)

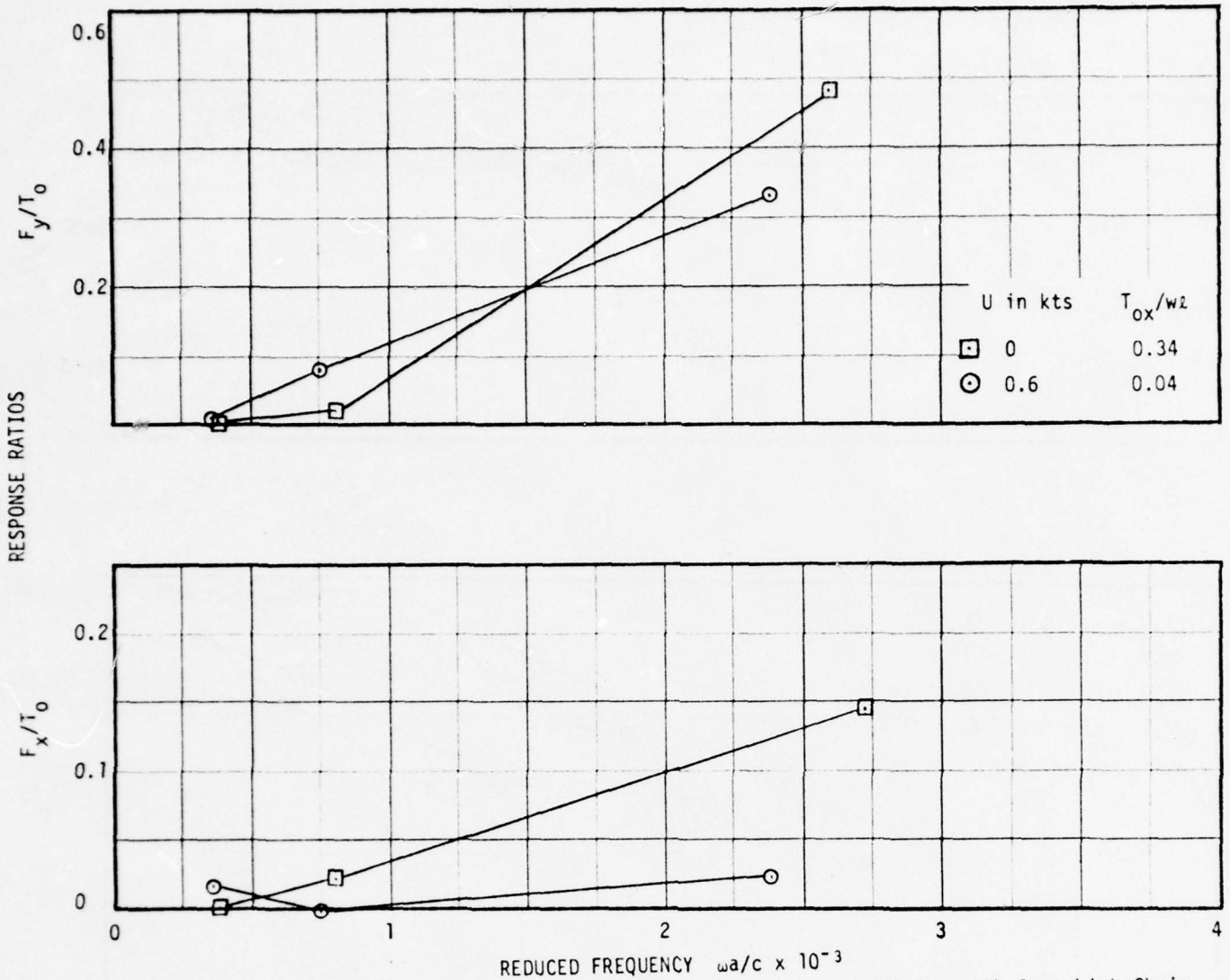

Figure 13 - Dynamic Load Response to Vertical Motion on Weighted Nylon with Open-Link Chain on the Bottom (ℓ = 12.05 feet, Bottom Anchor)

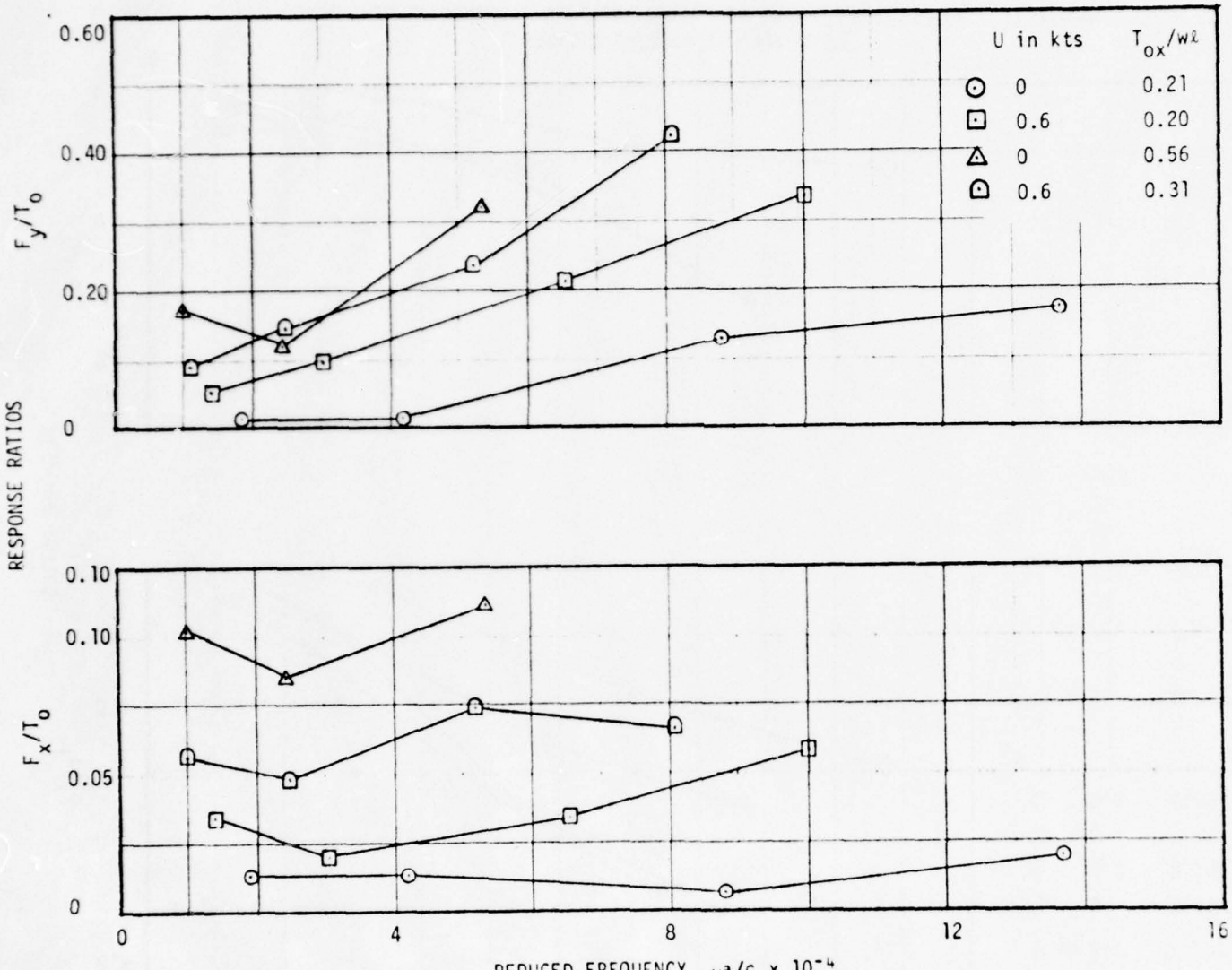

Figure 14 - Dynamic Load Response to Vertical Motion on Open-Link Chain (ℓ = 9.9 feet, Fixed Pivot)

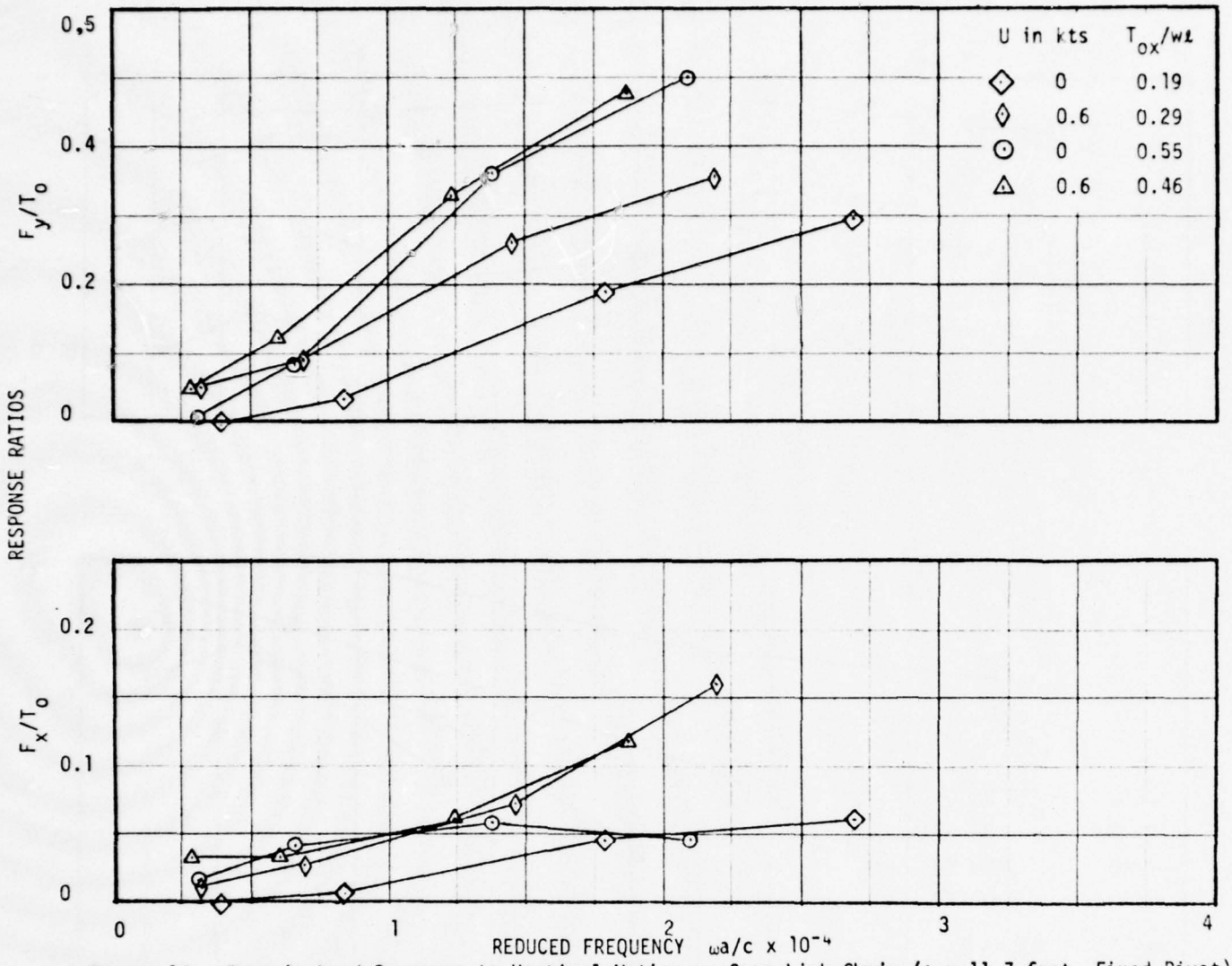

Figure 15 - Dynamic Load Response to Vertical Motion on Open-Link Chain (ℓ = 11.7 feet, Fixed Pivot)

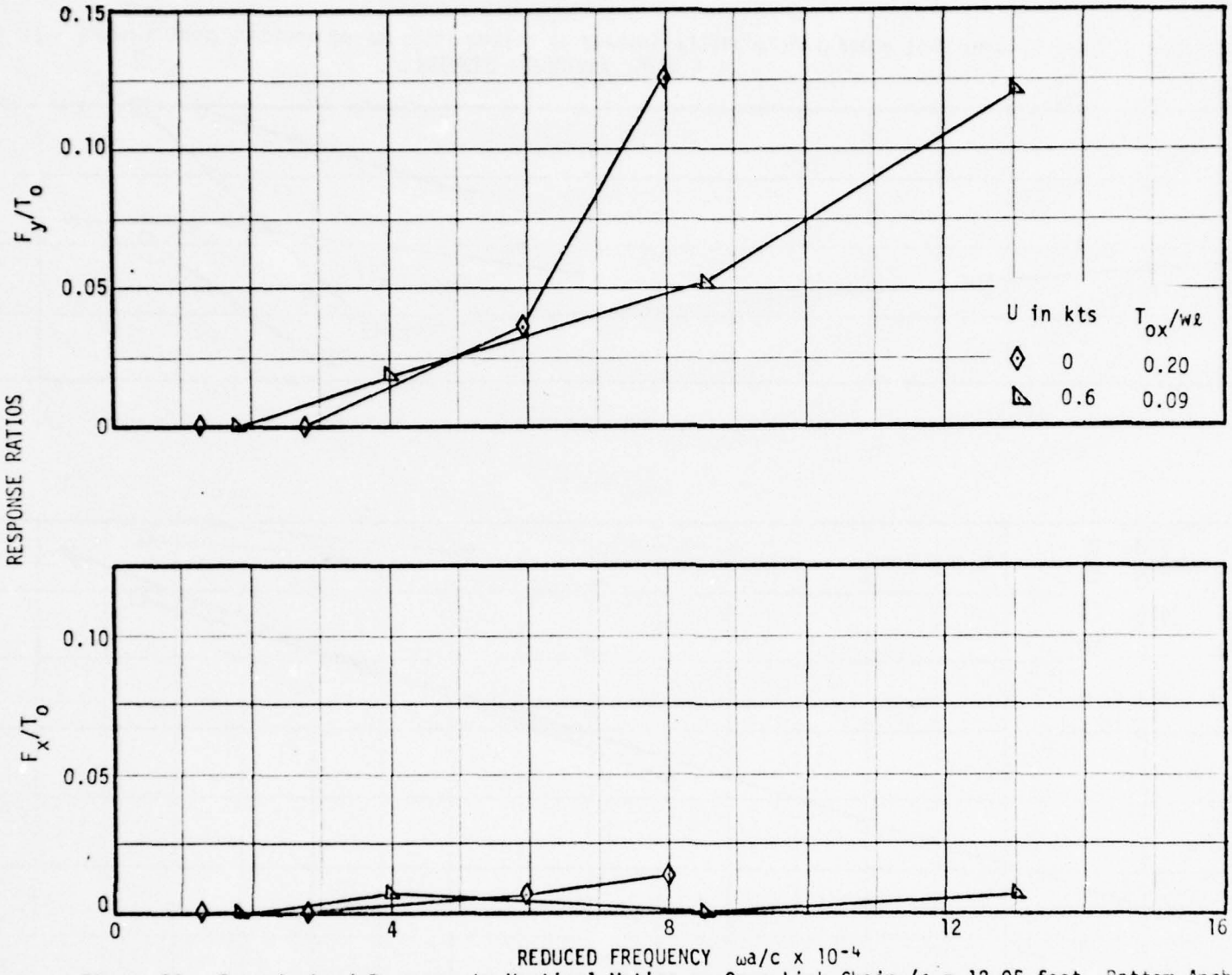

Figure 16 - Dynamic Load Response to Vertical Motion on Open-Link Chain (ℓ = 12.05 feet, Bottom Anchor)

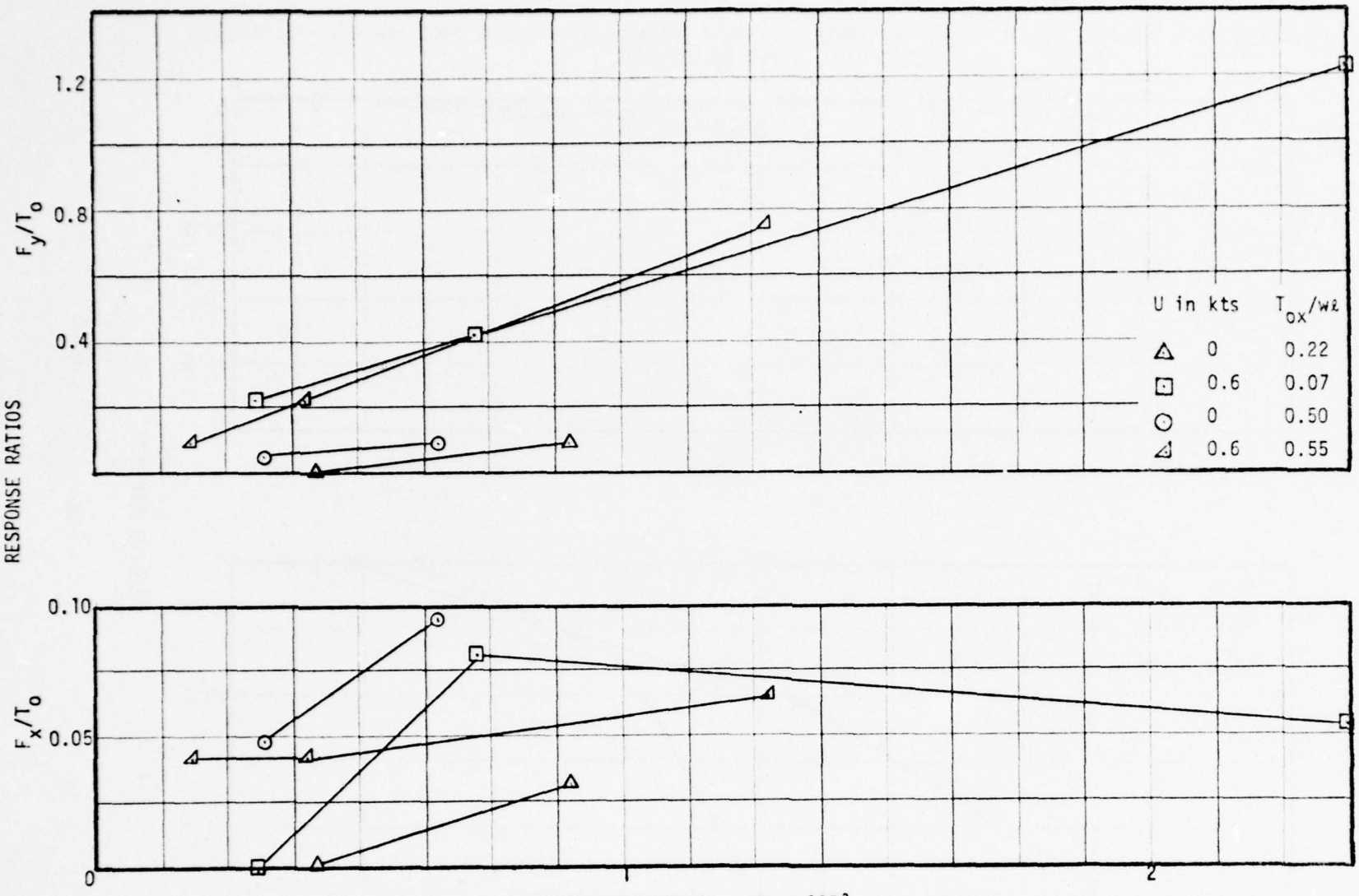

Figure 17 - Dynamic Load Response to Vertical Motion on Mercury-Filled Polyethylene Tube (ℓ = 10 feet, Fixed Pivot)

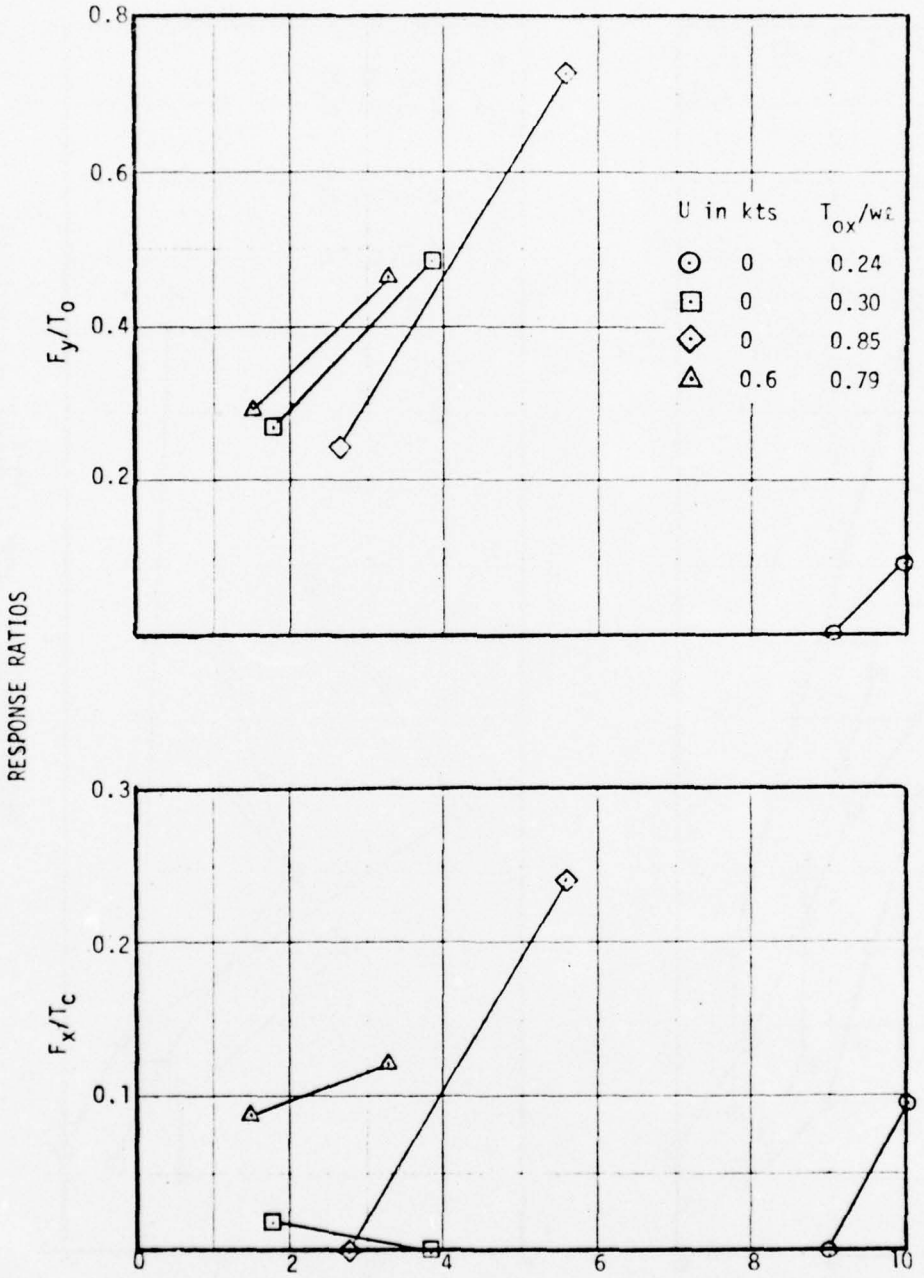

Figure 18 - Dynamic Load Response to Vertical Motion on Bead Chain (ℓ = 9.9 feet, Fixed Pivot)

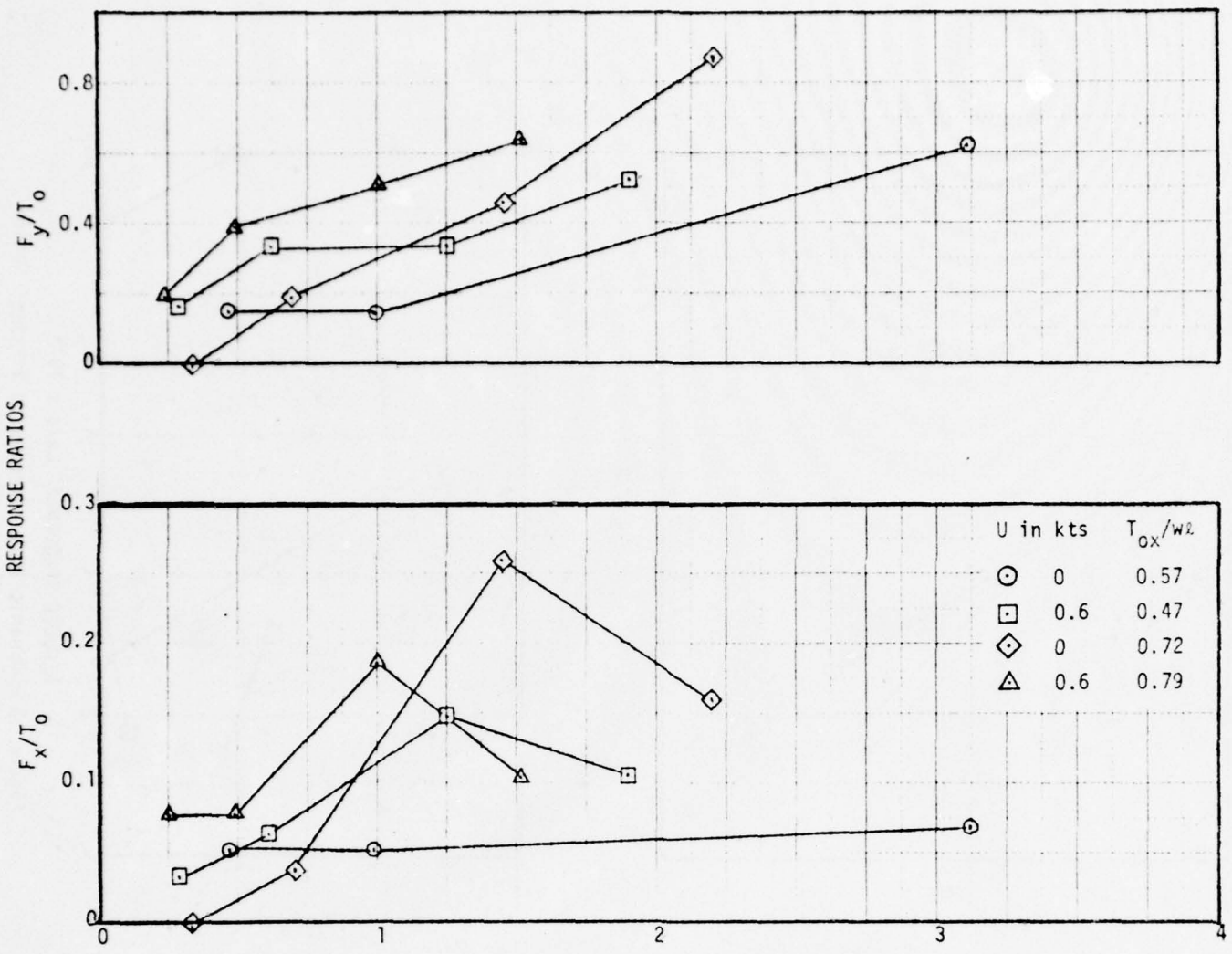

Figure 19 - Dynamic Load Response to Vertical Motion on Bead Chain
(ℓ = 11.7 feet, Fixed Pivot)

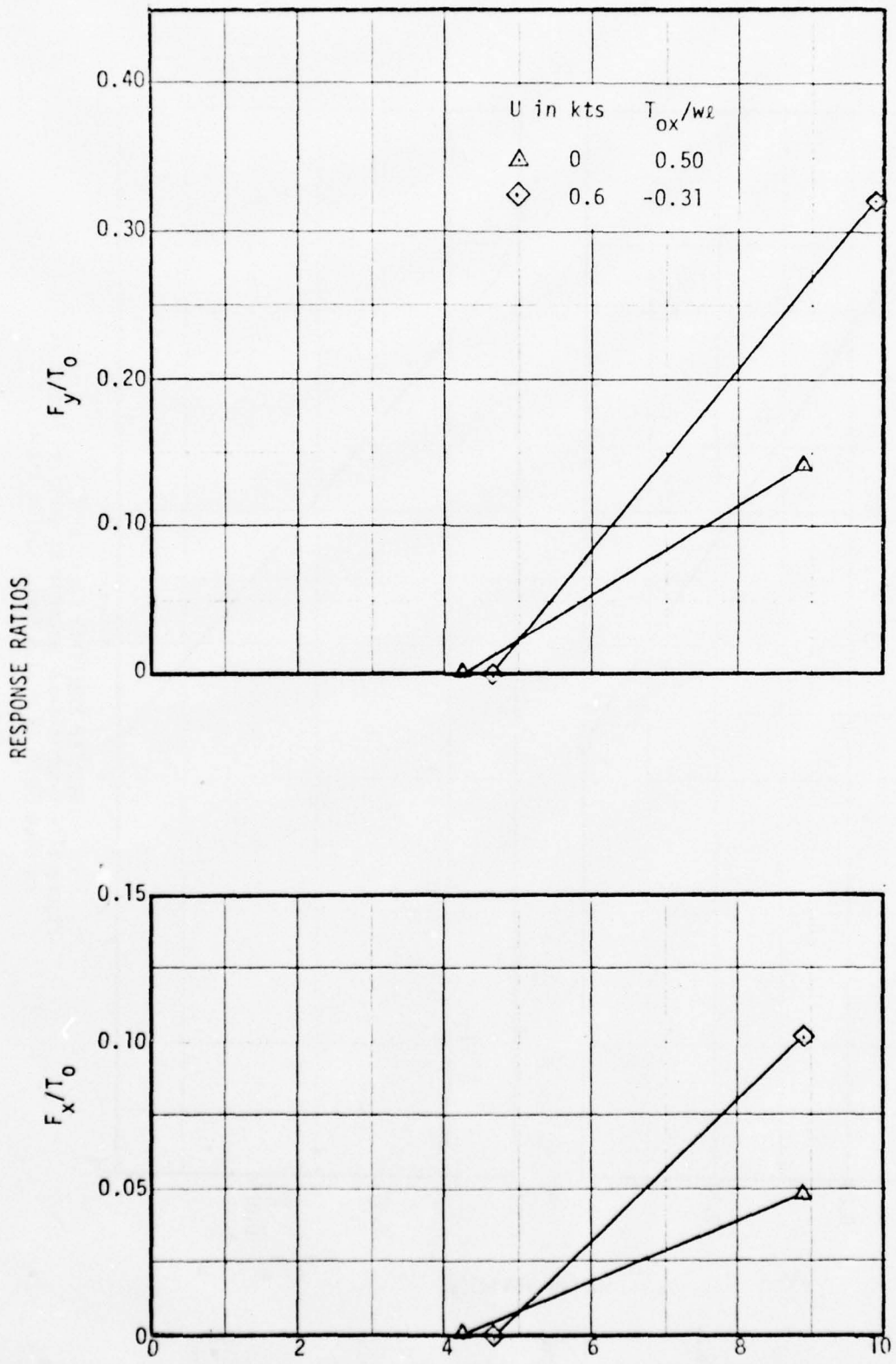

Figure 20 - Dynamic Load Response to Vertical Motion on Bead Chain (ℓ = 12.05 feet, Bottom Anchor)

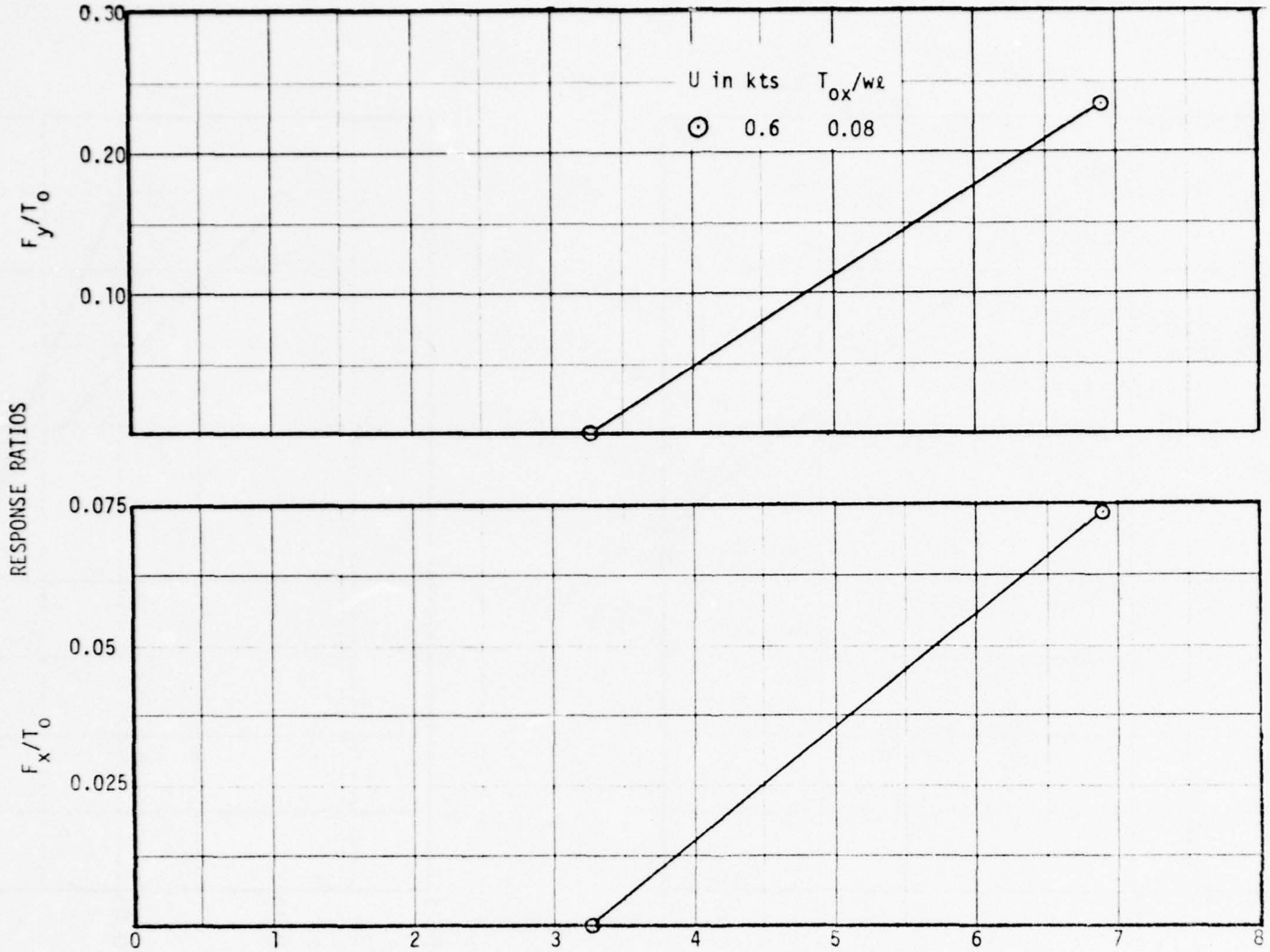

Figure 21 - Dynamic Load Response to Vertical Motion on Bead Chain (ℓ = 14.5 feet, Bottom Anchor)

Observations of motions in the mooring lines indicated differences in behavior between the different model moorings. All models exhibited motions in the plane of the steady-state catenary similar to those illustrated in Figure 22. In all cases the most severe changes in cable angle appeared at the fixed pivot, which was a reflection point for waves traveling up and down the mooring line. The wire rope and the mercury filled polyethylene tube, which were both stiff in bending, exhibited well defined nodal patterns with standing waves similar to the sketch shown in Figure 22. In traveling waves, the nodes move along the line; whereas, in standing waves, the nodes remain in fixed positions along the line. These patterns did not appear to change with frequency and, hence, the patterns probably were related to kinks in these lines rather than being results of resonance phenomena. The more flexible open-link chain, bead chain, and weighted cord models exhibited mostly traveling waves which began at the top, reflected from the fixed pivot, and returned to the top. The stiff models exhibited significant motion normal to the plane of the catenary, especially near the fixed pivot. The flexible models exhibited none of this out-of-plane motion, except for the weighted cord which exhibited a higher frequency small amplitude wiggle out-of-plane. This may have resulted because the cord was weighted with discrete masses in the form of lead shot. As a result, the out-of-plane wiggle could have been pendulus motion of these weights.

As to cases where mooring line was allowed to lie on the bottom, the motions were diminished by the removal of the fixed pivot which had acted as a wave reflector.

CONCLUSIONS AND RECOMMENDATIONS

In terms of the objectives of the above experimental program, the following conclusion is drawn:

1. The variety of conditions listed in Table 4 and Appendix A indicate that sufficient data were taken to validate the analytical methods for predicting the dynamic loads in mooring lines with forced vertical motions at the tops

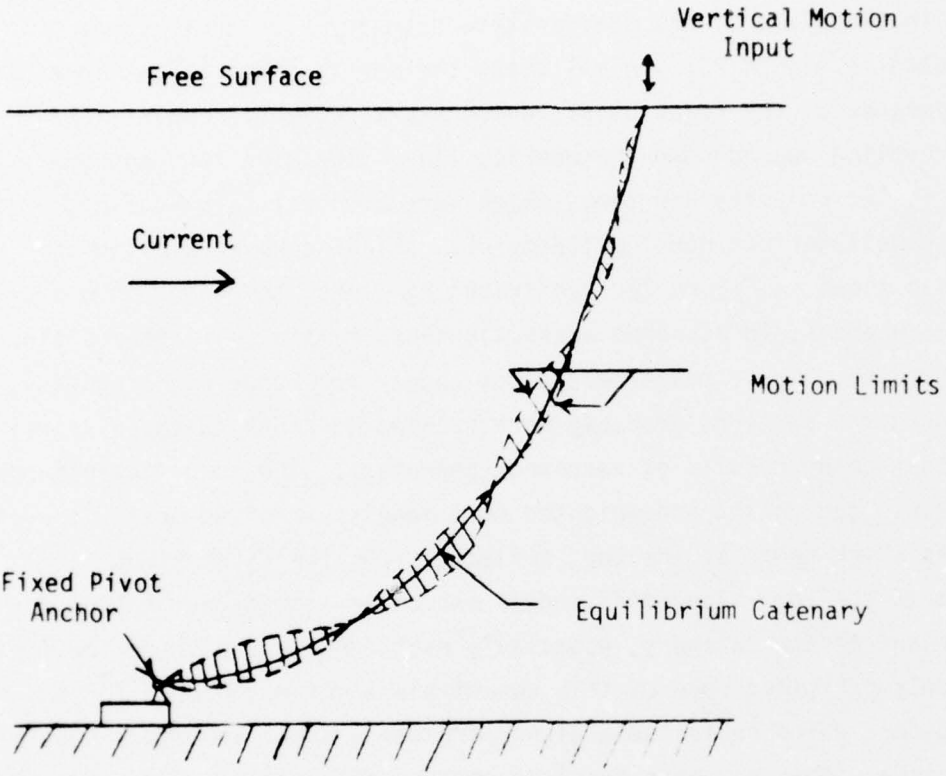

Figure 22 - Typical Motion Response in Plane of Model Mooring Catenary

of the mooring lines. Some of these data were used for validation in References 2 and 4. To complete the validation, however, data are needed with forced horizontal motions at the tops of the mooring lines.

Based on these experiments, the following conclusions are drawn:

1. In terms of ranges over which the dynamic responses are linear, that is where load responses to a sinusoidal motion input remain sinusoidal, motion amplitudes of 0.043 foot produced mostly linear responses; whereas, amplitudes of 0.109 foot produced mostly non-linear responses. Compared to the model mooring depth of 9 feet, both of these amplitudes are large. Also, non-linear effects increased with frequency and differ with mooring line material. Experiments with more amplitudes and frequencies are needed to better define the linear, dynamic response ranges.

2. Non-linear effects, such as out-of-plane motion, were observed on the models with bending stiffness, even when the dynamic load responses appeared linear.

3. For vertical motion input at the top of the model moorings, the horizontal and vertical load response ratios exhibited the following:

   a. Trends in the load response ratios with frequency shown in Figures 11 through 21 were similar to those expected from theory when the equilibrium tension is sufficiently large,[2]

   b. Preload effects were influenced by bending stiffness in that:

      (1) For the flexible models, load ratios increased with increased preload,

(2) For the stiff models, load ratios decreased with increased preload.

c. Load ratios increased with current, and

d. Load ratios decreased with increasing cable scope.

4. The motional responses of the model moorings were influenced by bending stiffness in that:

   a. The flexible models exhibited mostly traveling waves in the plane of the cable catenaries which were continuously reflected up and down the cable.

   b. The stiff models exhibited strong nodal motions with standing waves both in and out of the plane of the cable catenaries.

5. The stiff models also exhibited more tendencies toward distorted and highly peaked load responses than did the flexible models.

6. For deep sea moorings where the watch circle is to be minimized the above conclusions indicate that the best mooring line material is flexible in bending. The prototype lines shown in Figure 1 and 2 are flexible, with the added advantage that they also are extensible. Extensibility provides cushioning of otherwise large transient loads during deployment. Anchor chain is added to the bottoms of these systems to prevent chafing of the synthetic lines. Additionally, the experimental results indicate significantly reduced dynamic loads with the chain on the bottom.

Although some of the experimental results have been used to validate the prediction technique for dynamic responses presented in References 2 and 4, the weighted nylon cord results were not used, but the flexibility and extensibility of the weighted cord match the characteristics of the prototype mooring lines better than do the other models. Therefore, it is recommended that the weighted cord results be used to validate the dynamic prediction techniques.

For further validation of the prediction models, the following experiments are recommended:

1. Responses to horizontal motion input, which, when coupled with the vertical motion results, complete the description of the motional input expected from the buoy in a seaway,

2. Experiments with scope-to-depth ratios greater than 1.3 to determine the effects of scope on the dynamic load responses,

3. Experiments at several amplitudes of motion to determine effects of amplitude on dynamic load responses and to provide data for simulation of dynamic responses to motions of a buoy in a seaway with a spectrum of frequencies and amplitudes. For more accurate measurements, such experiments should use more sensitive load cells (within the state-of-the-art) placed at both top and bottom and full movie coverage of the mooring line with a background grid to measure motion.

4. Repeat experiments reported here with more accurate instrumentation to minimize uncertainties.

Once validated, the mooring dynamics prediction technique should be combined with the buoy motion model of Reference (3) to predict the actual responses of prototype moorings in realistic seaways and currents to assess such characteristics as maintenance of station and survivability.

REFERENCES

1. Snyder, R. M., "Buoys and Buoy Systems," in Section 9 of the Handbook of Ocean and Underwater Engineering, edited by J. J. Myers, C. H. Holm, and R. F. McAllister (New York: McGraw-Hill Book Company, (1969), pp. 9-81 thru 9-115.

2. Breslin, J. P., "Comparison of Two Sets of Calculated Model Cable Forces with Results from Measurements," prepared for Sperry Systems Management Division (January 1973).

3. Breslin, J. P., "Dynamic Forces Exerted by Oscillating Cables," Journal of Hydronautics, Vol. 8, No. 1, pp. 19-31 (January 1974).

4. Lee, C. A., "The Characteristics and Utilization of the David W. Taylor Model Basin Circulating Water Channel," Proceedings of the Third Hydraulics Conference, State University of Iowa, Studies in Engineering Bulletin 31 (June 1946).

5. Schreiber, H. G., Jr., "Hydrodynamics of Moored Buoys," paper presented at the Marine Technology Society 8th Annual Conference and Exposition (September 1972).

APPENDIX A

MEASURED DYNAMIC LOAD RESPONSES ON MODEL MOORINGS

TABLE A1 - MEASURED DYNAMIC LOADS IN RESPONSE TO VERTICAL MOTIONS ON A WEIGHTED NYLON CORD MODEL MOORING, ℓ = 9.9 FEET, FIXED PIVOT ANCHOR

Current, Knots	Horizontal Displacement, Feet	Frequency, Hertz	Dynamic Load		Run
			F_x Pounds	F_y Pounds	
0	3.76	0.40	0 $\pm$ 0.006	0 $\pm$ 0.006	148
		0.87	0.006 $\pm$ 0.006	0.019 $\pm$ 0.006	149
		1.81	0.029 $\pm$ 0.010	0.013 $\pm$ 0.017	150
		2.73	0.008 $\pm$ 0.007	0.106 $\pm$ 0.033	151
0.6	3.69	0.42	0.006 $\pm$ 0.006	0.031 $\pm$ 0.006	152
		0.90	0 $\pm$ 0.006	0.075 $\pm$ 0.006	153
		1.82	0.011 $\pm$ 0.008	0.098 $\pm$ 0.017	154
		2.76	0.002 $\pm$ 0.007	0.117 $\pm$ 0.034	155
0	4.02	0.42	0 $\pm$ 0.006	0 $\pm$ 0.006	156
		0.90	0.003 $\pm$ 0.006	0.016 $\pm$ 0.006	157
		1.84	0.007 $\pm$ 0.009	0.080 $\pm$ 0.016	158
		2.77	0.005 $\pm$ 0.008	0.062 $\pm$ 0.027	159
0.6	3.81	0.41	0.003 $\pm$ 0.006	0.041 $\pm$ 0.006	160
		0.90	0.009 $\pm$ 0.006	0.072 $\pm$ 0.006	161
		1.76	0.006 $\pm$ 0.009	0.144 $\pm$ 0.016	162
		2.70	0.008 $\pm$ 0.009	0.129 $\pm$ 0.010	163

TABLE A2 - MEASURED DYNAMIC LOADS IN RESPONSE TO VERTICAL MOTIONS ON A WEIGHTED NYLON CORD MODEL MOORING, ℓ = 11.7 FEET, FIXED PIVOT ANCHOR

Current, Knots	Horizontal Displacement, Feet	Frequency, Hertz	Dynamic Load F_x Pounds	Dynamic Load F_y Pounds	Run
0	6.23	0.40	0 ± 0.006	0 ± 0.006	113
		0.86	0.006 ± 0.006	0.006 ± 0.006	114
		2.72	0.005 ± 0.008	0.102 ± 0.033	116
0.6	6.61	0.42	0.003 ± 0.006	0.034 ± 0.006	117
		0.89	0 ± 0.006	0.050 ± 0.006	118
		1.82	0.007 ± 0.010	0.106 ± 0.017	119
		2.77	0.003 ± 0.008	0.113 ± 0.031	120
0	7.04	0.18	0.006 ± 0.006	0.006 ± 0.006	121
		0.28	0.006	0.006	122
		0.41	0.006	0.006	123
		0.52	0.003	0.009	124
		0.64	0.006	0.006	125
		0.75	0.006	0.006	126
		0.86	0.006	0.006	127
		0.99	0.003	0.016	128
		1.12	0	0.025	129
		1.22	0	0.025	130
		1.35	0.003	0.041	131
		1.46	0.012	0.037	132
		1.58	0.006	0.056	133
		1.82	0.022 ± 0.009	0.060 ± 0.016	135
		1.94	0.018 ± 0.009	0.071 ± 0.016	136
		2.06	0.015 ± 0.007	0.094 ± 0.022	137
		2.19	0.012 ± 0.007	0.083 ± 0.022	138
		2.30	0.012 ± 0.007	0.098 ± 0.023	139
		2.43	0.009 ± 0.006	0.113 ± 0.025	140
		2.55	0.011 ± 0.009	0.082 ± 0.031	141
		2.66	0.008 ± 0.007	0.106 ± 0.033	142
		2.77	0.009 ± 0.007	0.096 ± 0.035	143
0.6	6.88	0.41	0.006 ± 0.006	0.031 ± 0.006	144
		0.89	0.003 ± 0.006	0.066 ± 0.006	145
		1.83	0.009 ± 0.009	0.128 ± 0.015	146
		2.74	0.012 ± 0.007	0.145 ± 0.035	147

TABLE A3 - MEASURED DYNAMIC LOADS IN RESPONSE TO VERTICAL MOTIONS ON A WEIGHTED NYLON CORD PLUS CHAIN MODEL MOORING, ℓ = 12.05 FEET, BOTTOM ANCHOR

Current, Knots	Horizontal Displacement, Feet	Frequency, Hertz	Dynamic Load		Run
			F_x Pounds	F_y Pounds	
0	6.78	0.40	0 $\pm$ 0.006	0 $\pm$ 0.006	196
		0.85	0.006 $\pm$ 0.006	0.006 $\pm$ 0.006	197
		2.73	0.041 $\pm$ 0.007	0.137 $\pm$ 0.017	199
0.6	5.63	0.41	0.006 $\pm$ 0.006	0.006 $\pm$ 0.006	200
		0.87	0 $\pm$ 0.006	0.025 $\pm$ 0.006	201
		2.74	0.007 $\pm$ 0.007	0.104 $\pm$ 0.016	203

TABLE A4 - MEASURED DYNAMIC LOADS IN RESPONSE TO VERTICAL MOTIONS ON AN OPEN-LINK CHAIN MODEL MOORING, ℓ = 9.9 FEET, FIXED PIVOT ANCHOR

Current, Knots	Horizontal Displacement, Feet	Frequency, Hertz	Dynamic Load F_x Pounds	Dynamic Load F_y Pounds	Run
0	3.76	0.18	0.006 ± 0.006	0.006 ± 0.006	43
		0.41	0.006	0.006	44
		0.86	0.003	0.059	45
		1.34	0.009	0.078	46
0.6	3.69	0.19	0.022	0.034	50
		0.42	0.013	0.062	51
		0.90	0.022	0.134	52
		1.37	0.037	0.212	53
0	4.02	0.16	0.074	0.125	57
		0.38	0.062	0.087	58
		0.83	0.081	0.230	59
0.6	3.79	0.18	0.043	0.069	62
		0.41	0.037	0.112	63
		0.86	0.056	0.181	64
		1.33	0.050	0.325	65

TABLE A5 - MEASURED DYNAMIC LOADS IN RESPONSE TO VERTICAL MOTIONS ON AN OPEN-LINK CHAIN MODEL MOORING, ℓ = 11.7 FEET, FIXED PIVOT ANCHOR

Current, Knots	Horizontal Displacement, Feet	Frequency, Hertz	Dynamic Load F_x Pounds	Dynamic Load F_y Pounds	Run
0	6.23	0.38	0 ± 0.006	0 ± 0.006	164
		0.84	0.003 ± 0.006	0.016 ± 0.006	165
		1.78	0.021 ± 0.009	0.087 ± 0.014	166
		2.68	0.028 ± 0.008	0.138 ± 0.027	167
0.6	6.61	0.41	0.006 ± 0.006	0.031 ± 0.006	168
		0.88	0.016 ± 0.006	0.053 ± 0.006	169
		1.82	0.042 ± 0.010	0.150 ± 0.016	170
		2.76	0.094 ± 0.008	0.211 ± 0.032	171
0	7.04	0.41	0.009 ± 0.006	0.003 ± 0.006	172
		0.88	0.025 ± 0.006	0.050 ± 0.006	173
		1.82	0.035 ± 0.009	0.221 ± 0.013	174
		2.76	0.028 ± 0.008	0.308 ± 0.035	175
0	6.88	0.42	0.022 ± 0.006	0.034 ± 0.006	176
		0.89	0.022 ± 0.006	0.084 ± 0.006	177
		1.82	0.041 ± 0.009	0.226 ± 0.015	178
		2.74	0.081 ± 0.007	0.325 ± 0.018	179

TABLE A6 - MEASURED DYNAMIC LOADS IN RESPONSE TO VERTICAL MOTIONS ON AN OPEN-CHAIN MODEL MOORING, ℓ = 12.05 FEET, BOTTOM ANCHOR

Current, Knots	Displacement, Feet	Frequency, Hertz	Dynamic Load F_x Pounds	Dynamic Load F_y Pounds	Run
0	6.72	0.18	0 $\pm$ 0.006	0 $\pm$ 0.006	29
		0.41	0	0	30
		0.87	0.003	0.016	31
		1.32	0.006	0.056	32
0.6	5.73	0.19	0	0	36
		0.42	0.003	0.009	37
		0.90	0	0.025	38
		1.36	0.003	0.059	39

TABLE A7 - MEASURED DYNAMIC LOADS IN RESPONSE TO VERTICAL MOTION ON A MERCURY-FILLED POLYETHYLENE TUBE MOORING MODEL, ℓ = 10 FEET, FIXED PIVOT ANCHOR

Current, Knots	Horizontal Displacement, Feet	Frequency, Hertz	Dynamic Load		Run
			F_x Pounds	F_y Pounds	
0	3.80	0.41	0 $\pm$ 0.006	0 $\pm$ 0.006	97
		0.88	0.003	0.009	98
0.6	3.73	0.39	0	0.025	101
		0.83	0.009	0.047	102
		2.70	0.006 $\pm$ 0.007	0.137 $\pm$ 0.026	104
0	4.06	0.41	0.006 $\pm$ 0.006	0.006 $\pm$ 0.006	105
		0.84	0.012	0.012	106
0.6	3.85	0.41	0.009	0.021	109
		0.88	0.009	0.047	110
		2.78	0.014 $\pm$ 0.007	0.161 $\pm$ 0.028	112

TABLE A8 - MEASURED DYNAMIC LOAD IN RESPONSE TO VERTICAL MOTION ON A BEAD CHAIN MODEL MOORING, ℓ = 9.9 FEET, FIXED PIVOT ANCHOR

Current, Knots	Horizontal Displacement, Feet	Frequency, Hertz	Dynamic Load F_x Pounds	Dynamic Load F_y Pounds	Run
0	3.76	0.41	0 $\pm$ 0.006	0 $\pm$ 0.006	81
		0.86	0.006	0.006	82
0.6	3.69	0.42	0.003	0.041	85
		0.89	0	0.075	86
0	4.02	0.41	0	0.025	89
		0.86	0.025	0.075	90
0.6	3.81	0.42	0.016	0.053	93
		0.89	0.022	0.084	94

TABLE A9 - MEASURED DYNAMIC LOAD IN RESPONSE TO VERTICAL MOTION AS A BEAD CHAIN MODEL MOORING, ℓ = 11.7 FEET, FIXED PIVOT ANCHOR

Current, Knots	Horizontal Displacement, Feet	Frequency, Hertz	Dynamic Load		Run
			F_x Pounds	F_y Pounds	
0	6.23	0.41	0.003 ± 0.006	0.009 ± 0.006	180
		0.86	0.003	0.009 ± 0.006	181
		2.72	0.004	0.045 ± 0.018	183
0.6	6.61	0.41	0.003	0.016 ± 0.006	184
		0.88	0.006	0.031 ± 0.006	185
		1.80	0.014 ± 0.009	0.032 ± 0.016	186
		2.74	0.010 ± 0.007	0.050 ± 0.017	187
0	7.04	0.40	0 ± 0.006	0 ± 0.006	188
		0.85	0.003 ± 0.006	0.016 ± 0.006	189
		1.78	0.021 ± 0.009	0.038 ± 0.015	190
		2.70	0.013 ± 0.007	0.071 ± 0.033	191
0.6	6.88	0.42	0.009 ± 0.006	0.022 ± 0.006	192
		0.89	0.009 ± 0.006	0.047 ± 0.006	193
		1.81	0.022 ± 0.010	0.060 ± 0.016	194
		2.72	0.012 ± 0.006	0.076 ± 0.018	195

TABLE A10 - MEASURED DYNAMIC LOAD IN RESPONSE TO VERTICAL MOTION ON A BEAD CHAIN MODEL MOORING, ℓ = 12.05 FEET, BOTTOM ANCHOR

Current, Knots	Horizontal Displacement, Feet	Frequency, Hertz	Dynamic Load		Run
			F_x Pounds	F_y Pounds	
0	6.38	0.41	0 $\pm$ 0.006	0 $\pm$ 0.006	69
		0.86	0.003	0.009	70
0.6	2.82	0.41	0	0	73
		0.88	0.006	0.019	74

TABLE A11 - MEASURED DYNAMIC LOAD IN RESPONSE TO VERTICAL MOTION ON A BEAD CHAIN MODEL MOORING, ℓ = 14.5 FEET, BOTTOM ANCHOR

Current, Knots	Displacement, feet	Frequency, Feet	Dynamic Load F_x Pounds	Dynamic Load F_y Pounds	Run
0.6	8.88	0.40	0 $\pm$ 0.006	0 $\pm$ 0.006	77
		0.84	0.006 ↓	0.019 ↓	78

TABLE A12 - MEASURED DYNAMIC LOAD IN RESPONSE TO VERTICAL MOTION ON A WIRE ROPE MODEL MOORING, ℓ = 9.9 FEET, FIXED PIVOT ANCHOR

Current, Knots	Horizontal Displacement, Feet	Frequency, Hertz	Dynamic Load F_x Pounds	Dynamic Load F_y Pounds	Run
0	3.76	0.16	0 $\pm$ 0.006	0 $\pm$ 0.006	15
		0.39	0	0	16
		0.87	0.003	0.025	17
		1.34	0.009	0.047	18
0.6	3.69	0.19	0.006	0.031	22
		0.42	0.009	0.047	23
		0.89	0.016	0.078	24
		1.36	0.009	0.122	25

DTNSRDC ISSUES THREE TYPES OF REPORTS

(1) DTNSRDC REPORTS, A FORMAL SERIES PUBLISHING INFORMATION OF PERMANENT TECHNICAL VALUE, DESIGNATED BY A SERIAL REPORT NUMBER.

(2) DEPARTMENTAL REPORTS, A SEMIFORMAL SERIES, RECORDING INFORMATION OF A PRELIMINARY OR TEMPORARY NATURE, OR OF LIMITED INTEREST OR SIGNIFICANCE, CARRYING A DEPARTMENTAL ALPHANUMERIC IDENTIFICATION.

(3) TECHNICAL MEMORANDA, AN INFORMAL SERIES, USUALLY INTERNAL WORKING PAPERS OR DIRECT REPORTS TO SPONSORS, NUMBERED AS TM SERIES REPORTS, NOT FOR GENERAL DISTRIBUTION.